



HAL
open science

Porous polymers and metallic nanoparticles: A hybrid wedding as a robust method toward efficient supported catalytic systems

Romain Poupart, Daniel Grande, Benjamin Carbonnier, Benjamin Le Droumaguet

► To cite this version:

Romain Poupart, Daniel Grande, Benjamin Carbonnier, Benjamin Le Droumaguet. Porous polymers and metallic nanoparticles: A hybrid wedding as a robust method toward efficient supported catalytic systems. *Progress in Polymer Science*, 2019, 96, pp.21-42. 10.1016/j.progpolymsci.2019.05.003 . hal-02157146

HAL Id: hal-02157146

<https://hal.science/hal-02157146>

Submitted on 5 Jul 2021

HAL is a multi-disciplinary open access archive for the deposit and dissemination of scientific research documents, whether they are published or not. The documents may come from teaching and research institutions in France or abroad, or from public or private research centers.

L'archive ouverte pluridisciplinaire **HAL**, est destinée au dépôt et à la diffusion de documents scientifiques de niveau recherche, publiés ou non, émanant des établissements d'enseignement et de recherche français ou étrangers, des laboratoires publics ou privés.

Porous Polymers and Metallic Nanoparticles: a Hybrid Wedding as a Robust Way Toward Efficient Supported Catalytic Systems

*Romain Poupart, Daniel Grande, Benjamin Carbonnier, Benjamin Le Droumaguet**

Université Paris Est, Institut de Chimie et des Matériaux Paris-Est (ICMPE), UMR 7182, CNRS, UPEC, F- 94320 THIAIS France

Submitted as a review article to *Progress in Polymer Science*

* Corresponding author: Dr. Benjamin Le Droumaguet

Phone: +33 (0)1 49 78 11 77

Fax: +33 (0)1 49 78 12 08

E-mail: ledroumaguet@icmpe.cnrs.fr

Abstract: Over the past recent years, nanoparticles have been the subject of numerous studies, due to their unique intrinsic properties. In particular, they have found widespread interest in heterogeneous catalysis, and their development in this area is growing. Nevertheless, they still display drawbacks and, among them, the question of their recyclability may arise. In order to avoid tedious filtration steps, metallic nanoparticles may be advantageously supported on miscellaneous porous materials. Polymer materials can be envisaged as versatile and effective supports, due to their low production cost and easy functionalization. This review will first focus on different types of porous polymers developed in view of their further use as catalytic supports. Then, a brief description of the nanoparticles synthesis will be addressed, before a presentation of typical examples reported in the literature about metallic nanoparticles immobilized on porous polymers meant for heterogeneous supported catalysis.

Keywords: Porous polymers; Metallic nanoparticles; Hybrid materials; Supported heterogeneous catalysis

Abbreviations

AM	acrylamide
ATRP	atom transfer radical polymerization
BCP	block copolymer
BET	Brunauer-Emmett-Teller
BJH	Barrett-Joyner-Halenda
CEC	capillary electrochromatography
DABCO	1,4-diazabicyclo[2.2.2]octane
DMF	<i>N,N</i> -dimethylformamide
DMSO	dimethylsulfoxide
DSC	differential scanning calorimetry
DSDMA	disulfide-based dimethacrylate (bis(2-methacryloyl)oxyethyl disulfide)
DTT	D,L-dithiothreitol
EGDMA	ethylene glycol dimethacrylate
GCMA	glycerol carbonate methacrylate
GMA	glycidyl methacrylate
HEMA	2-hydroxyethyl methacrylate
HIPE	high internal phase emulsion
IUPAC	International union of pure and applied chemistry
MIP	mercury intrusion porosimetry
NAS	<i>N</i> -acryloxysuccinimide
NMR	nuclear magnetic resonance
NP	nanoparticle; PAA, poly(acrylic acid)
PEI	poly(ethylene imine)

PES	poly(ether sulfone)
PI	polyisoprene
PLA	poly(D,L-lactide)
PMMA	poly(methyl methacrylate)
PS	polystyrene
PVA	poly(vinyl alcohol)
RAFT	reversible addition-fragmentation chain transfer
ROMP	ring opening metathesis polymerization
ROP	ring opening polymerization
SEM	scanning electron microscopy
TEOS	tetraethyl orthosilicate
TFA	trifluoroacetic acid
THF	tetrahydrofuran
TIPS	temperature-induced phase separation
TON	turnover number
UV	ultraviolet
VBC or 4-VBC	4-vinylbenzyl chloride
VDMA	2-vinyl-4,4-dimethylazlactone

Contents

1	Introduction.....	1
2	Porous polymers: general features, synthesis, and characterization	5
2.1	Basics on porous polymers	5
2.2	Macroporous polymers	5
2.3	Nanoporous polymers.....	10
2.4	Biporous polymers.....	18
2.5	Characterization techniques of porous materials.....	23
3	Application of metallic nanoparticle immobilized on porous polymers as supported catalysts	27
3.1	Key features of nanoparticles	27
3.2	Nanoparticles supported by macroporous polymers	31
3.3	Nanoparticles supported by nanoporous polymers.....	40
3.4	Nanoparticles supported by biporous polymers	46
4	Critical appraisal of the different strategies	50
5	Conclusions and prospects	53
	Acknowledgments	54
	References	55

1 **1 Introduction**

2 A catalyst is commonly described by the International Union of Pure and Applied
3 Chemistry (IUPAC) as a substance that increases the rate of a reaction without modifying the
4 overall standard Gibbs energy change in the reaction. Two different types of catalytic
5 processes actually exist: (i) one type based on homogeneous catalysis, namely the catalyst is
6 present in the same phase as the reactants, mostly a liquid phase [1], while (ii) the other type
7 is named as heterogeneous when the catalyst and the reactants are in different phases.
8 Though, the frontier between both kinds of processes can be sometimes really thin in
9 particular cases [2]. The metal-based catalyst is mostly in the solid state, finely divided, and
10 the reactants are in the liquid or gaseous one. Nevertheless, some examples of heterogeneous
11 biphasic catalysis reported that the catalyst remains in one liquid phase (*i.e.* water) and
12 reactants in another one (*i.e.* oil), such as for the hydroformylation of propene, for instance
13 [3]. One such example illustrates very well the possibility to perform catalysis by phase
14 transfer. Recent developments in this research area notably demonstrated that catalytic
15 reactions, especially organometallic-based ones, can be carried out in more environmentally-
16 friendly conditions than a few years ago [4]. Such catalytic reactions more and more call upon
17 green and sustainable chemistry, and efforts have been put forward in this direction to address
18 specific issues related to the recycling of the catalysts.

19 In this context, supported metallic nanoparticles present some undeniable advantages
20 regarding heterogeneous catalysis. They have actually shown an increasing interest over the
21 last decade. Such nanometer-sized metallic particles, immobilized on high surface area
22 materials, can now be relatively well characterized by different techniques and have shown
23 some great catalytic performances. The preparation of such hybrid materials involves the
24 design and development of still novel and efficient catalysts, and thus the improvement of
25 (in)organic supports in terms of specific surface area, porosity, surface functionality and

1 chemical inertness towards a wide variety of versatile or harsh reaction conditions [5].
2 Catalytic systems are commonly used in various industrial techniques [6] as well as in our
3 common life, as demonstrated by automotive catalytic converters for instance [5]. While a
4 serious drawback has been encountered with suspended nanoparticles, *i.e.* the recycling of the
5 nanometal catalyst through time-consuming and non-environmentally friendly purification
6 processes, miscellaneous solutions exist. First, a recently reported solution to address this
7 issue relies on the use of nanoparticles bearing a magnetic core, generally γ -Fe₂O₃. In this
8 case, the nanometal recovery step can be achieved by harvesting with the help of a magnet.
9 However, a coating (silica, carbon, or polymer) of these magnetic metallic nanoparticles is
10 generally required to allow for their suspension in a stable fashion, thus avoiding their
11 coalescence, and protecting them from the surrounding environment. When a polymer coating
12 is implemented for such magnetic nanoparticles, the resulting coated particles are not stable in
13 harsh reaction conditions, such as at high temperature. The same observations have been
14 made with silica coatings that are porous. Such an inorganic coating has a very low stability in
15 harsh pH conditions. Finally, when carbon-based coatings are used for magnetic
16 nanoparticles, they aim at agglomerating and form clusters, which would lead to a decrease of
17 specific surface area of the catalysts [7]. Then, another solution consists in using macroscopic
18 porous matrices as supports for the immobilization of metallic nanoparticles at the pore
19 surface. The robust and straightforward immobilization of nanoparticles at the pore surface of
20 suitable supports, notably by tuning the nature of the interface, enables to further avoid
21 tedious purification processes, as the supported catalyst can be readily removed from the
22 reaction mixture by mere filtration.

23 Hybrid catalysts based on supported metallic nanoparticles generally consist of
24 (in)organic/hybrid porous frameworks presenting a rather high specific surface area that
25 allows for a large amount of metallic nanoparticles to be immobilized in a straightforward and

1 robust fashion. Among such high specific surface area supports, inorganic materials like
2 zeolites [8] or ordered mesoporous silicas [9] can be found. Zeolites possess pores within the
3 microporous range, enabling them to be used as catalyst supports in liquid or gas reaction
4 conditions. Even though zeolites can be synthesized in rather mild temperature conditions
5 (90–180 °C), their preparation requires pressures up to 15 bars in autoclaves. Other inorganic
6 supports like mesoporous silicas can be prepared in a straightforward fashion by reacting in a
7 first step a surfactant typically arising from the Tween[®] or Pluronic[®] family and a precursor
8 mainly tetraethyl orthosilicate (TEOS) in mild conditions [10]. However, the major concern
9 of such porous inorganic supports relies on the harsh reaction conditions required in the
10 calcination step that enables for the disappearance of the organic surfactant and thus the
11 generation of the porosity. The calcination step is indeed performed at very high temperatures,
12 *i.e.* hundreds of °C, for several hours, which is highly energy- and time-consuming. On the
13 other hand, organic polymer-based supports as well as modified carbon nanotubes [11] have
14 been recently developed. Finally, hybrid structures, *i.e.* Metal-Organic Frameworks [12]
15 (MOFs) have been more recently deeply investigated in heterogeneous supported catalysis
16 applications, due to their versatility and remarkably high surface area. Unfortunately, this
17 class of hybrid materials suffers from high fabrication costs, poor selectivity, low capacity,
18 and difficulty in recycling/regeneration [13].

19 In the case of polymeric materials, some advantages rapidly come to mind. They can
20 first be easily functionalized so as to tune the pore surface chemistry, which is of utmost
21 importance for further adsorption of chemical species or metallic nanoparticles. One can also
22 easily play with the hydrophilic/hydrophobic nature of the polymer interface that will have
23 some consequences on the interaction with the surrounding fluid, notably in terms of
24 wettability. The porosity can also be readily varied in terms of pore size, ratio, and shape.
25 Such polymeric materials are generally cross-linked, allowing for a better stability of the

1 resulting hybrids in miscellaneous experimental conditions such as harsh pH or temperature.
2 Finally, such polymer-based porous supports have mechanical properties tunable in a useful
3 range, and their production cost is lower than that of their inorganic analogues. On the
4 opposite, some drawbacks can be noticed with such porous polymers: they cannot generally
5 resist to high pressure and temperature, rendering some catalytic chemical reactions on these
6 supports difficult to envision. However, they still remain common porous supports for
7 metallic nanoparticles immobilization and are thus the subject of widespread interest in the
8 field of heterogeneous catalysis.

9 In light of this general introduction, this review will focus on the design and synthesis
10 of hybrid materials consisting of metallic nanoparticles immobilized at the pore surface of
11 porous polymers for catalytic reaction purposes. A first section will be devoted to general
12 features about porous polymer-based materials; then the main strategies to prepare such
13 porous supports and the associated techniques of characterization will be presented. The
14 reader should bear in mind that this section will not give a full overview of all strategies
15 implemented for the synthesis of porous polymers, but it will rather focus on those mainly
16 used for the preparation of porous polymeric systems meant for supported catalysis
17 applications. It is thus recommended for casual readers to refer to more general reviews on
18 porous polymers to get a full overview of their preparation routes [14]. A second section will
19 then be directed towards the use of hybrid porous materials obtained after metallic
20 nanoparticles immobilization at the pore surface of polymeric supports, and their further
21 implementation in heterogeneous catalysis.

22

1 **2 Porous polymers: general features, synthesis, and characterization**

2 **2.1 Basics on porous polymers**

3 According to the IUPAC [13], porous solid materials can be classified into three main
4 categories. Firstly, microporous materials are characterized by pore diameters below 2 nm.
5 Secondly, the term “mesoporous” is used to qualify materials with pore diameters between 2
6 and 50 nm. Finally, macroporous materials can be distinguished by a pore diameter larger
7 than 50 nm. It is at this stage very important to note that this classification is the only one that
8 is commonly admitted by the scientific community. However, in the areas of materials science
9 and nanotechnologies, the term “nanoporous” is commonly applied to materials containing
10 pore sizes lower than 100 nm, even though such a terminology can be somehow confusing for
11 casual readers and even experts in the field. Likewise, materials with porosity in the
12 micrometer range (or more) are often called macroporous materials. This general
13 classification can be applied to any type of porous material, namely inorganic, hybrid or
14 organic ones.

15

16 **2.2 Macroporous polymers**

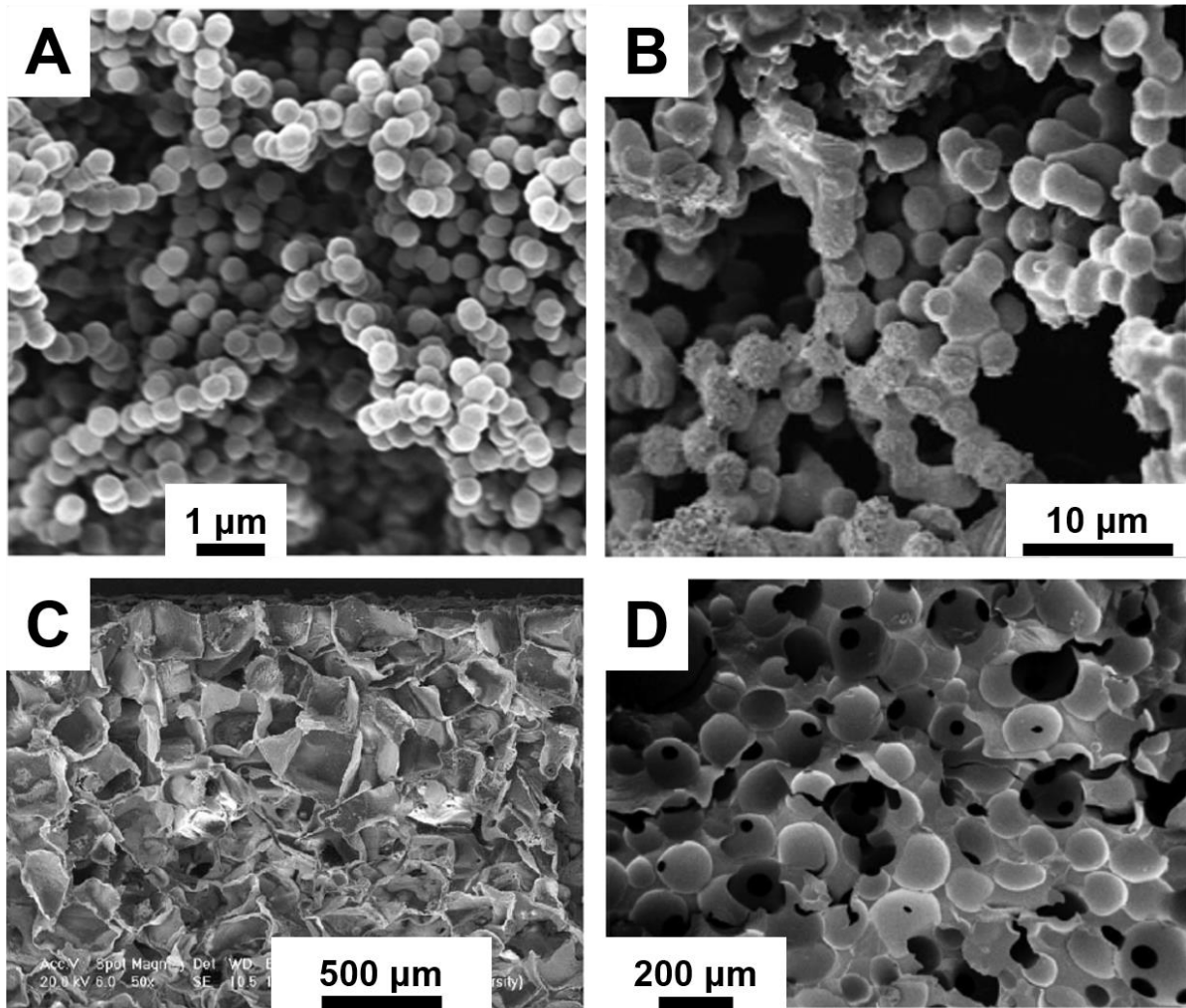
17 Macroporous materials may be prepared by different techniques through the use of
18 miscellaneous porogens. In 1967, Seidl *et al.* [15] distinguished three main synthetic
19 strategies to prepare porous polymeric matrices: (i) by using a porogenic solvent, (ii) by using
20 a non-solvent as the porogen or (iii) by adding a linear polymer as a macromolecular porogen.
21 According to Švec and Fréchet, these synthetic strategies are the most commonly used, but
22 above all they are easy to implement [16].

23 When a solvent is used as a porogenic agent, the initiator, monomer(s) and cross-
24 linker are dissolved in a solvent or in a solvent mixture. When the polymerization is triggered
25 by photochemical or thermal decomposition of the initiator, polymeric particles nucleate,

1 grow, and coalesce in the solvent. Depending on the affinity of the solvent for the growing
2 cross-linked polymer, the former will be ejected more or less promptly from the polymer
3 matrix through a syneresis phenomenon, creating voids filled with solvent. Upon porogenic
4 solvent removal, these voids generate the porosity within the polymeric material. As the
5 moment of the solvent ejection is closely related to the solvent and polymer compatibility, the
6 pore size of the resulting materials can be thus easily tuned by merely changing the solvent
7 polarity. In addition, the porosity ratio will also be dictated by the comonomers/(co)solvent(s)
8 volume ratio. Finally, the porosity can be open or closed, depending on the amount of
9 porogenic agent chosen. For very low porogenic solvent(s) to (co)monomers ratio, it is
10 particularly true.

11 Such a way of generating porosity within polymeric materials has been widely
12 implemented notably for preparing polymer-based monolithic columns with an interconnected
13 porosity. This enables liquids or gases to easily flow through such monolithic columns,
14 depending on the average pore size of the material as well as on the viscosity of the solvent, to
15 avoid too high back pressures. Different monolithic columns have been prepared so far
16 following this synthetic strategy, whatever the nature of the monomer used. Generally, the
17 monomer is functional, that is to say it possesses a chemical moiety that can be easily
18 chemically modified through a post-polymerization step consisting of a reaction occurring at
19 the interface of the pore with the surrounding fluid, allowing for the interfacial properties of
20 the pore surface to be easily tuned. Historically, the first monolithic capillaries were prepared
21 by Švec's research group in the mid-1990's using glycidyl methacrylate (GMA) as a
22 functional monomer [17]. GMA bears an epoxide moiety that can be easily functionalized
23 through ring-opening reaction with rather strong nucleophiles like amines [17]. Later on, the
24 same research group has deeply expanded his pioneering works on the exploitation of GMA
25 monomer, notably for chromatographic applications [18]. It is now used in other laboratories

1 [19, 20], allowing for a plethora of potential applications to be envisioned. In the late 1990's,
2 4-chloromethyl styrene, also known as 4-vinylbenzyl chloride (4-VBC or VBC), was
3 investigated in applications related to monolithic columns [21]. This styrenic monomer gave
4 birth to highly hydrophobic columns, while the pore surface of the resulting materials can be
5 easily tuned by nucleophilic substitution of the benzylic chlorine. It is worth mentioning that
6 such functionalization reactions can lead to hypercrosslinked materials, provided that the
7 chemical graft to anchor possesses two identical reactive groups [22]. 2-Vinyl-4,4-
8 dimethylazlactone (VDMA) is another interesting monomer used for the preparation of
9 porous materials [23]. Indeed, VDMA can be readily incorporated into the composition of
10 polymerization mixtures in conjunction with diverse hydrophilic monomers, *e.g.* 2-
11 hydroxyethyl methacrylate (HEMA) and acrylamide (AM), to prepare functional in-capillary
12 monoliths that can be functionalized with amine bearing bio(macro)molecules [23]. Finally,
13 *N*-acryloxysuccinimide (NAS) and glycidyl carbonate methacrylate (GCMA) have been more
14 recently implemented for the design of innovative functional porous in-capillary columns, as
15 shown in **Fig. 1A** [24]. NAS can undergo nucleophilic substitution due to the presence of
16 pendant activated ester moieties and has been widely used for chromatographic applications,
17 such as capillary electrochromatography (CEC) separations [25-30] or for flow through
18 catalysis applications [31]. Alternatively, oligomeric or polymeric chains have also been used
19 as porogens in other studies (**Fig. 1B**) [32, 33].



1

2 **Fig. 1.** Examples of macroporous polymeric materials derived from the use of porogenic
 3 agents. (A) *N*-acryloylsuccinimide-based monoliths obtained in the presence of a porogenic
 4 solvent. [24], Copyright 2007 (Reproduced with permission from Elsevier Ltd). (B)
 5 polystyrene macroporous monolith obtained after leaching of a semi-interpenetrated
 6 polycaprolactone oligomer. [32], Copyright 2010 (Reproduced with permission from Elsevier
 7 Ltd). (C) Poly(D,L-lactic-*co*-glycolic acid)-based frameworks using NaCl cubic particles as
 8 macroporogens [34]. Copyright 2005. Reproduced with permission from Elsevier Ltd. (D)
 9 Porous poly(2-hydroxyethyl methacrylate) material obtained upon removal of sintered
 10 poly(methyl methacrylate) beads as 3-D macroporogenic template. [35], Copyright 2014
 11 (Reproduced with permission from Elsevier Ltd).

12

13 Other porogens than those defined by Seidl and coworkers are nowadays commonly
 14 used for different purposes. Especially, macroporogen templating has gained a tremendous

1 interest in the last years. It relies on the use of a so-called template which acts as a
2 macroporogen. It is added to the initial polymerization mixture (consisting of the initiator, the
3 (co)monomer(s) and the cross-linker(s)) and immediately removed after the polymerization
4 completion. The judicious choice of this porogenic template notably allows for tuning the
5 pore morphology as the pores will present a shape that perfectly matches the template imprint.
6 Such porogenic templates are based on solid, mostly inorganic crystal particle, such as sodium
7 chloride (NaCl) [36], calcium carbonate (CaCO₃) [37] or ammonium bicarbonate (NH₄HCO₃)
8 [36] particles, for instance. The use of such a methodology presents some non-negligible
9 advantages as it permits to vary the size (by particle sieving) and morphology (depending on
10 the shape of selected porogen) of the pores, while their removal is generally simple to achieve
11 through easy template leaching into an appropriate aqueous solution. In fact, they are usually
12 dissolved in pure water through particle leaching, such as for the extraction of NaCl particles.
13 Alternatively, CaCO₃ particle-based templates require an acidic aqueous solution to be
14 removed from the polymer matrix. It is worth mentioning that the porogenic template could
15 also be prepared with the desired shape [34] (**Fig. 1C**). As a matter of fact, other
16 investigations reported on the use of different sacrificial templates derived from organic
17 (macro)molecules, such as paraffin or poly(methyl methacrylate) (PMMA) beads. In this case,
18 the porogen could also be dissolved *via* Soxhlet extraction with an appropriate organic
19 solvent. LaNasa *et al.* [38] and Le Droumaguet *et al.* [35] independently demonstrated that it
20 is possible to successfully use sintered polymeric PMMA beads as an original porogenic
21 template (**Fig. 1D**). Such sintered PMMA beads could further be extracted in organic
22 solvent(s), while the porous polymeric matrix remains intact, due to permanent cross-linking.
23 These sintered spherical beads allowed for the generation of interconnected spherical pores
24 upon removal of the macroporogen.

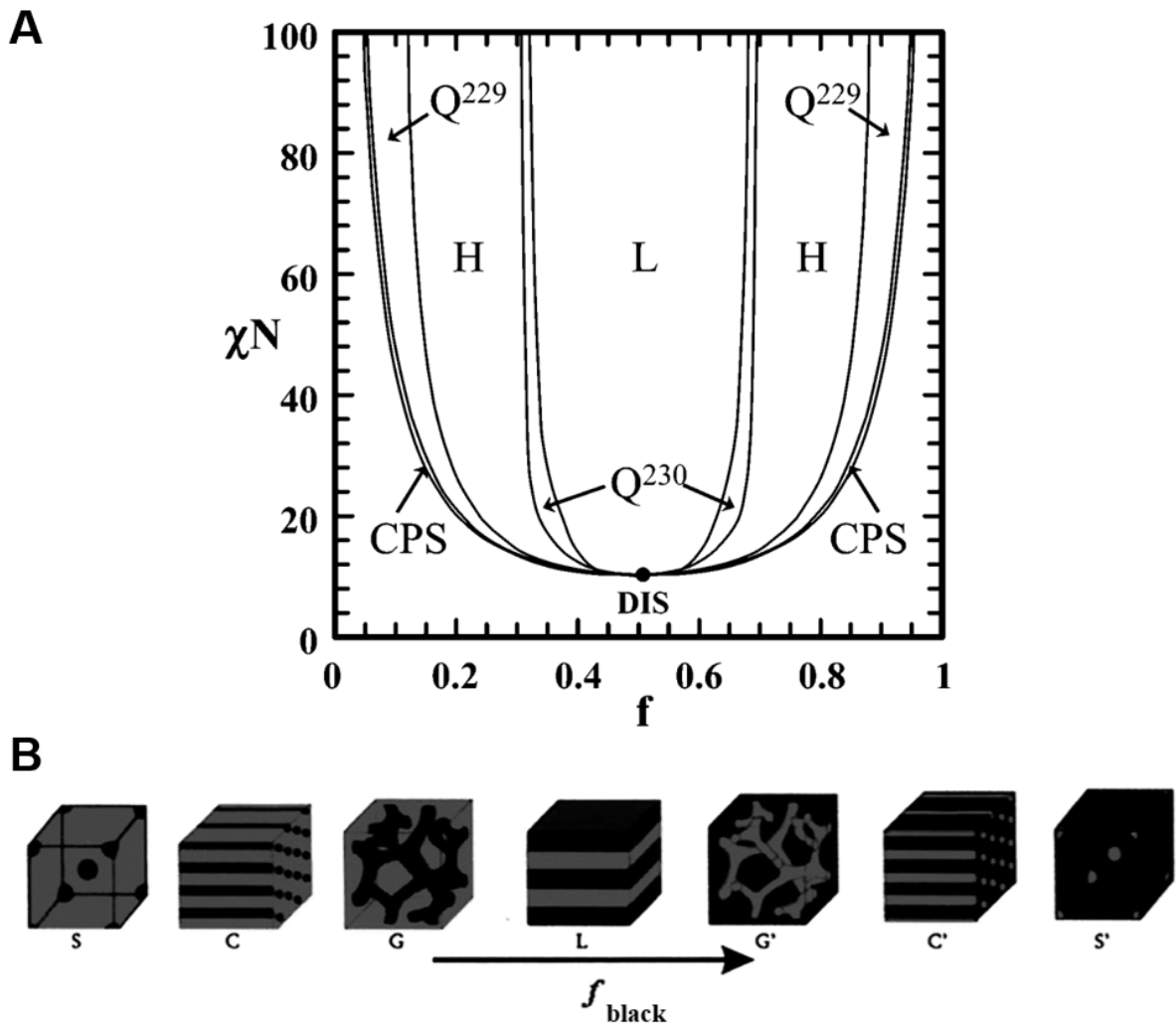
25

1 **2.3 Nanoporous polymers**

2 Miscellaneous approaches have been developed so far to prepare nanoporous polymer-
3 based materials. These materials are mostly used as filtration membranes. In this particular
4 case, the process is subtler than for the preparation of macroporous materials, and it usually
5 involves the removal of a sacrificial polymer segment from nanostructured precursors, thus
6 generating pores at the nanoscale level. Techniques like track-etching which lead to
7 nanopores will not be addressed here, but reviews discussing the subject may be easily found
8 [39].

9 A largely investigated strategy consists in specifically removing one sacrificial block
10 from oriented block copolymers (BCPs), thus leading to ordered nanoporous materials *via* a
11 process milder than that used with other strategies. BCPs and especially diblock copolymers
12 develop very precise equilibrium domain morphologies depending on three main critical
13 parameters, *i.e.* the volume fraction of both blocks f , the number of repeating units N in the
14 copolymer, and χ_{AB} the Flory-Huggins interaction parameter between the two different blocks
15 [40]. According to theoretical phase diagrams, body-centered spheres, hexagonally close-
16 packed cylinders, bicontinuous gyroids or alternating lamellae can be obtained (**Fig. 2**) [41,
17 42]. Polydispersity of both blocks is also a key parameter to precisely control the morphology
18 of the block copolymers after orientation of the nanodomains. Indeed, a high polydispersity of
19 the minority block has been shown to lead to a change of morphology due to a larger
20 interfacial curvature [43]. On the opposite, a high polydispersity of the majority one was
21 demonstrated to lead to a change of morphology due to a smaller interfacial curvature. So far,
22 different natures of sacrificial blocks have been implemented to prepare nanoporous materials
23 from this strategy. Historically, the first diblock copolymer precursors used were constituted
24 of a degradable polyisoprene (PI) block and of a stable polystyrene-derived (4-
25 vinylphenyl)dimethyl-2-propoxysilane) block, both synthesized by anionic polymerization.

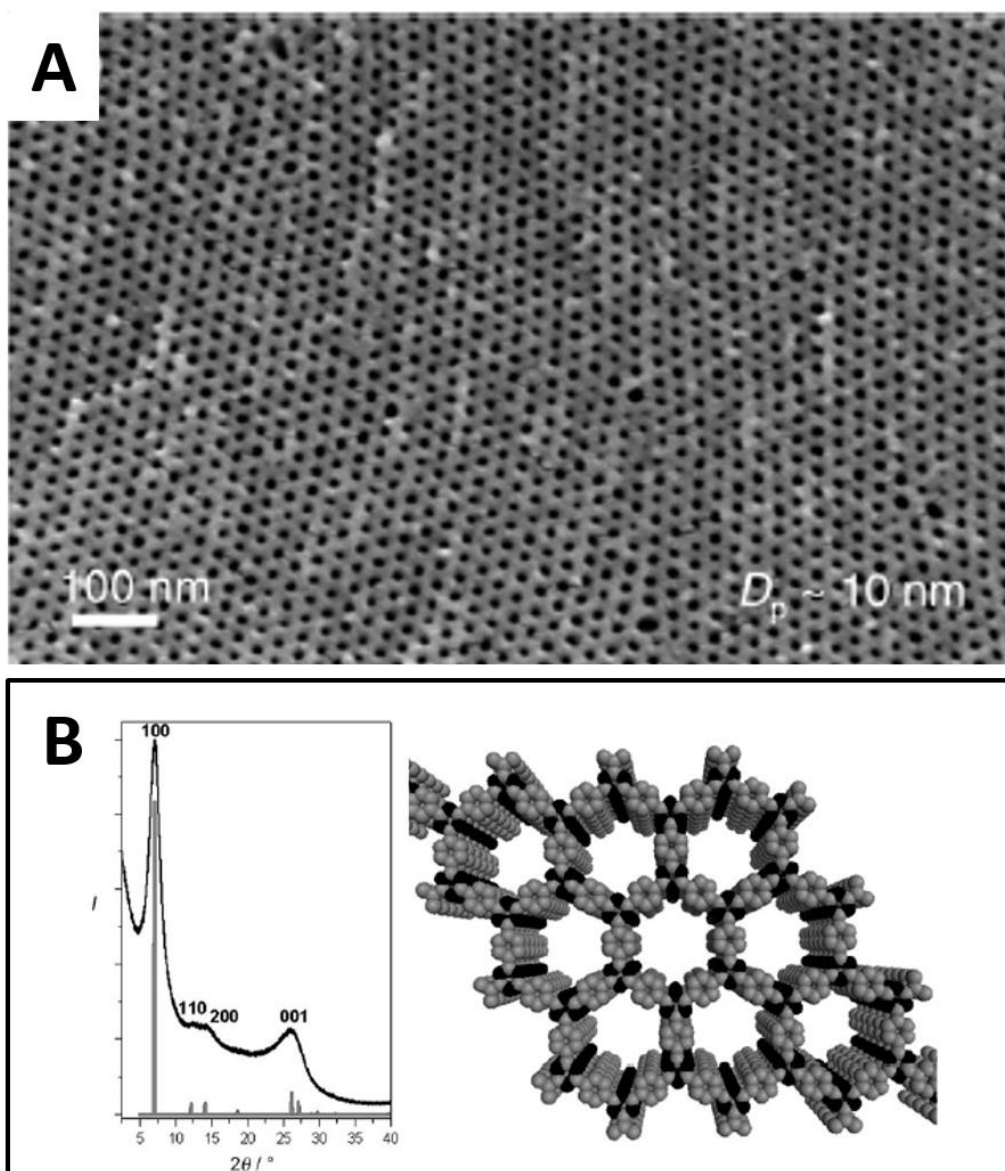
1 The former block was removed by ozonolysis that selectively cleaved the carbon-carbon
 2 double bonds of the isoprene units, while the polystyrene (PS) segment was simultaneously
 3 crosslinked, thus revealing nanoporous PS-based networks [44]. Later on, other research
 4 groups have successfully developed other sacrificial blocks by varying the conditions of
 5 etching [45]. Herein, we will focus on poly(D,L-lactide) (PLA), which has been widely used
 6 in the area of nanoporous polymers.



7
 8 Fig. 2. (A) Morphology diagram of AB diblock copolymers obtained upon orientation of
 9 respective BCP domains depending on the segregation regime (χN) and the volume fraction of
 10 the minor component (f): L, H, Q²²⁹, Q²³⁰, CPS and DIS stand for lamellae, hexagonally
 11 packed cylinders, spherical phases with $Im\bar{3}m$, 3D gyroid phase, close-packed (fcc or
 12 hexagonal) symmetry, or disorder respectively. [42], Copyright 2006 (Reproduced with
 13 permission from the American Chemical Society). (B) Schematic representation of the various

1 possible morphologies depending on f_{black} : S and S', C and C', G and G', L and L' stand for
2 spheres, cylinders, gyroids and lamellae, respectively. [41], Copyright 1999 (Reproduced with
3 permission from the American Institute of Physics).

4
5 PLA can be synthesized *via* anionic or coordinative ring-opening polymerization
6 (ROP) of 3,6-dimethyl-1,4-dioxane-2,5-dione (usually called D,L-lactide), from alcohol- [46]
7 or amine-based [47] initiators in the presence of organic [48] or organo-metallic [49]
8 catalysts. PLA is generally etched in mild conditions, namely in alkaline conditions and
9 especially in NaOH or KOH hydro-alcoholic solutions, as described by numerous studies
10 from Hillmyer and coworkers first in 2001 [50] or later on from our research group [51, 52]
11 (**Fig. 3A**). It is worth noticing that PLA can also be degraded in acidic conditions. It is not
12 until recently that such etching conditions have been reported in the literature for PS-*b*-PLA
13 [53].



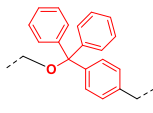
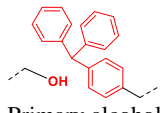
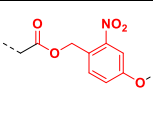
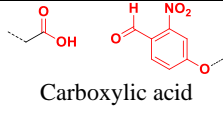
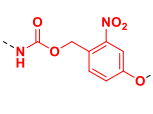
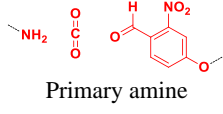
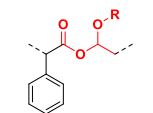
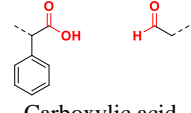
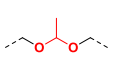
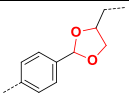
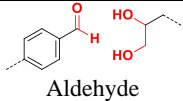
1
 2 **Fig. 3.** Examples of nanoporous polymeric materials. (A) Nanopores arising from selective
 3 hydrolysis of the PLA sacrificial block in a PS-*b*-PLA diblock copolymer. [51], Copyright
 4 2011 (Reproduced with permission from Elsevier Ltd). (B) Nanopores arising from an
 5 intrinsically microporous polytriazine network. [54], Copyright 2008 (Reproduced with
 6 permission from Wiley-VCH publishers).

7
 8 Another somehow smarter strategy to etch the sacrificial block from BCPs relies on
 9 the selective cleavage of the junction present between both block. Indeed, the degradable
 10 character of such a junction can lead to easy and straightforward removal of the entire
 11 sacrificial block in a non-solvent of the remaining block. Such a strategy notably permits to

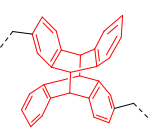
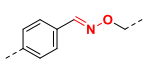
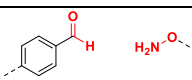
1 carry out the sacrificial block removal in milder conditions than those employed for the
2 chemical degradation of the block itself and to ensure the presence of a well-defined
3 functional group at the pore surface. Russell's group pioneered this elegant strategy by
4 precisely positioning an anthracene photodimer at the junction between both blocks of a
5 polystyrene-*block*-poly(methyl methacrylate), the PMMA sacrificial block being further
6 released from the oriented diblock copolymers by dissociation of the photodimer under UV or
7 thermal stimuli, thus revealing nanopores [55]. Later on, different selectively cleavable
8 chemical junctions have been used in diblock copolymers. They can be categorized into three
9 main sub-classes. The first one relies on using an irreversibly cleavable junction between both
10 blocks (**Table 1**). Trityl ether [56, 57] which is easily cleavable by trifluoroacetic acid (TFA),
11 *o*-nitrobenzyl ester [58-60] or carbamate [61] derivative, hemiacetal junction [62] or acetal
12 moiety [63, 64] for instance have been successfully implemented in this context. Other
13 strategies involving reversible junctions have also been put forward, such as the
14 aforementioned $[4\pi+4\pi]$ anthracene photodimer [55, 65], disulfide bridges, [66, 67] oxo-
15 imines [68] or hetero Diels-Alder adducts arising from RAFT agents [69], for instance, as
16 depicted in **Table 2**. Finally, other investigations reported on the possibility to implement
17 supramolecular junctions to link both blocks in a non-covalent manner, as shown in **Table 3**.
18 We can notably mention the use of terpyridine-ruthenium [70] or terpyridine-nickel [71]
19 complexes, ionic interactions [72] or even hydrogen bonds [73] taking place between the two
20 adjacent blocks of oriented copolymers.

21
22
23
24

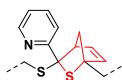
1 **Table 1.** Irreversibly cleavable junctions used for the preparation of functionalized
 2 nanoporous polymers.

Type of block junction	Junction chemical structure	Cleavage agent/stimulus	Chemical function remaining after cleavage	References
Trityl ether		Brønsted or Lewis acid (ex: TFA)	 Primary alcohol	[56, 57]
<i>o</i> -nitrobenzyl ester		UV light ($\lambda = 350$ nm)	 Carboxylic acid	[58-60, 74]
<i>o</i> -nitrobenzyl carbamate		UV light ($\lambda = 300$ nm)	 Primary amine	[61]
Hemiacetal ester		TFA	 Carboxylic acid	[62]
Acetal		TFA	 Alcohol	[64]
Acetal		TFA	 Aldehyde	[63]

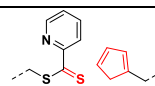
3
 4 **Table 2.** Reversible junctions used for the preparation of functionalized nanoporous
 5 polymers.

Type of block junction	Junction formula	Cleavage agent/stimulus	Chemical function remaining after cleavage	References
[4 π +4 π] anthracene photodimer		UV light ($\lambda = 280$ nm) 130-200 °C	 Anthracene	[55, 65]
Disulfide bridge		DTT, TPP or glutathione	 Thiol	[66, 67]
Oxi-imines		TFA	 Primary amine	[68]

Hetero Diels-
Alder adduct



110 °C



[69]

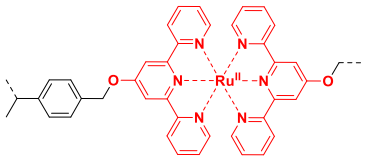
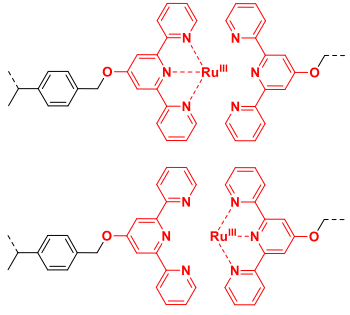
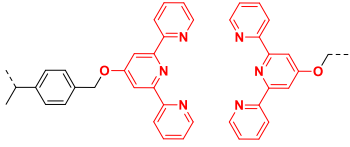
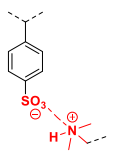
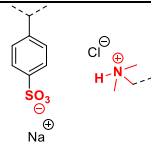
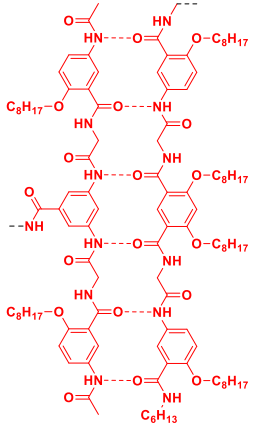
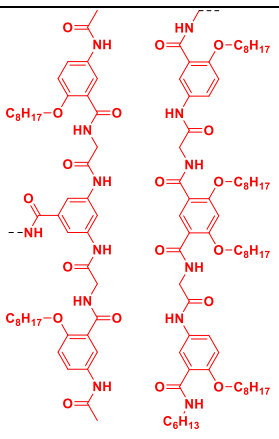
Thio-carbonyl-thio RAFT agent

1

2 Finally, some polymeric materials develop intrinsic free volume that can be viewed as
3 micropores; this is the so-called intrinsic microporosity. Such micropore sizes notably allow
4 such types of material to be used for gas-related applications [75-77] especially for separation
5 sciences, gas storage or heterogeneous catalysis in the gaseous phase. Only monomers that
6 offer a good rigidity to the polymer network can prevent them from pore collapse and enable
7 a permanent microporosity. Polymeric microporous polycyanurate [78], polyisocyanurate
8 [79], polyurethane [80], polytriazine [54] (**Fig. 3B**), based on Tröger's base [81] or porous
9 aromatics frameworks [82, 83] can be found among such innovative materials.

10

1 **Table 3.** Supramolecular junctions used for the preparation of functionalized nanoporous
 2 polymers.

Type of block junction	Junction formula	Cleavage agent	Chemical function remaining after cleavage	References
Terpyridine-ruthenium complexes		Ce(SO ₄) ₂ /H ₂ SO ₄ solution (pH = 1)	 Terpyridine ligand	[70]
Terpyridine-nickel complexes		KCN	 K ₂ [Ni(CN) ₄] Terpyridine ligand	[71]
Ionic interactions		NaCl in MeOH/H ₂ O solution	 Sulfonate	[72]
Hydrogen bonds donor-acceptor		H ₂ O/MeOH (50/50 % v/v) followed by CHCl ₃	 Hydrogen bond building block	[73]

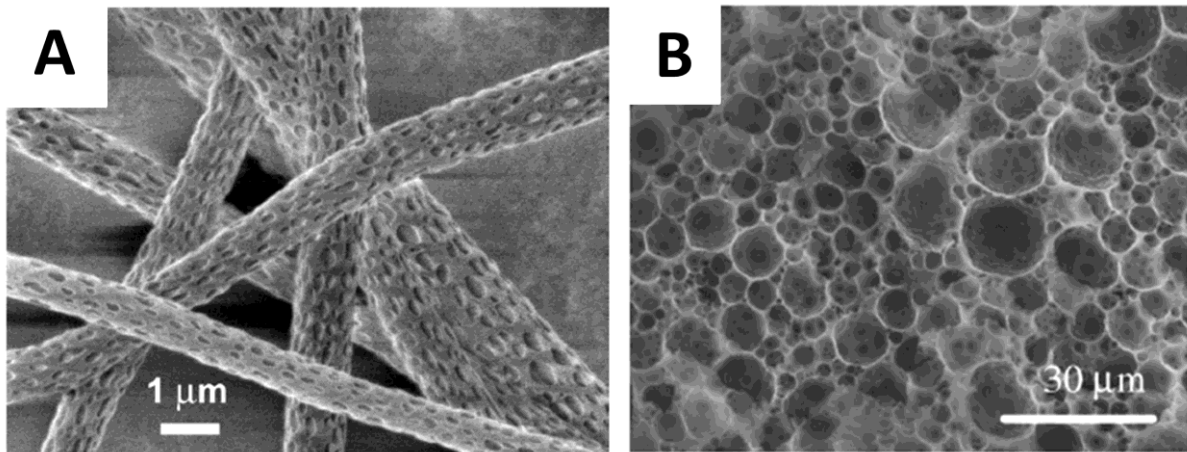
1 **2.4 Biporous polymers**

2 Biporous materials have gained a tremendous interest within the last decades in
3 different research area, such as civil engineering, tissue engineering or even drug delivery.
4 Scientists are now able to prepare porous polymers possessing at least two distinct levels of
5 porosity. Several methods have been so far developed to prepare biporous materials, including
6 rapid prototyping (also called solid free-form fabrication or additive manufacturing) which is
7 undergone by 3D printing [84], gas foaming [85], temperature-induced phase separation
8 (TIPS) [86], the polyHIPE technique or the double porogen templating approach. Due to
9 purpose considerations, this part will essentially focus on electropun materials, polyHIPEs,
10 and doubly porous materials derived from the double porogen templating approach, as these
11 three strategies were recently implemented in the literature for the preparation of hybrid
12 polymer-based materials dedicated to supported catalysis.

13 Closely related to the use of a 3-D printer (*i.e.* rapid prototyping) for constructing
14 biporous materials, electrospinning is a powerful technique that allows for the formation of
15 highly porous scaffolds from solutions of polymeric materials [87]. The electrospinning
16 process was patented by Anton Formhals in 1934 [88], and it was intensively developed by
17 Reneker's research group [89, 90] in the 1990's and 2000's with the emergency of
18 nanotechnologies. Electrospun materials are prepared by applying a high voltage electrostatic
19 field (usually in the 10-30 kV range) between a syringe containing a viscous polymeric
20 solution and a collector for the deposition of polymeric fibers. Due to the fiber packing, pores
21 with a wide pore size distribution are generated between fibers, thus allowing for the
22 production of macroporous materials with highly interconnected voids and a large ratio of
23 surface area to volume [91]. Electrospun polymeric fibers present morphological similarities
24 as natural collagen fibrils, and their morphologies can be easily tuned by varying different
25 parameters, such as the voltage, the syringe needle-to-collector distance, the polymer solution

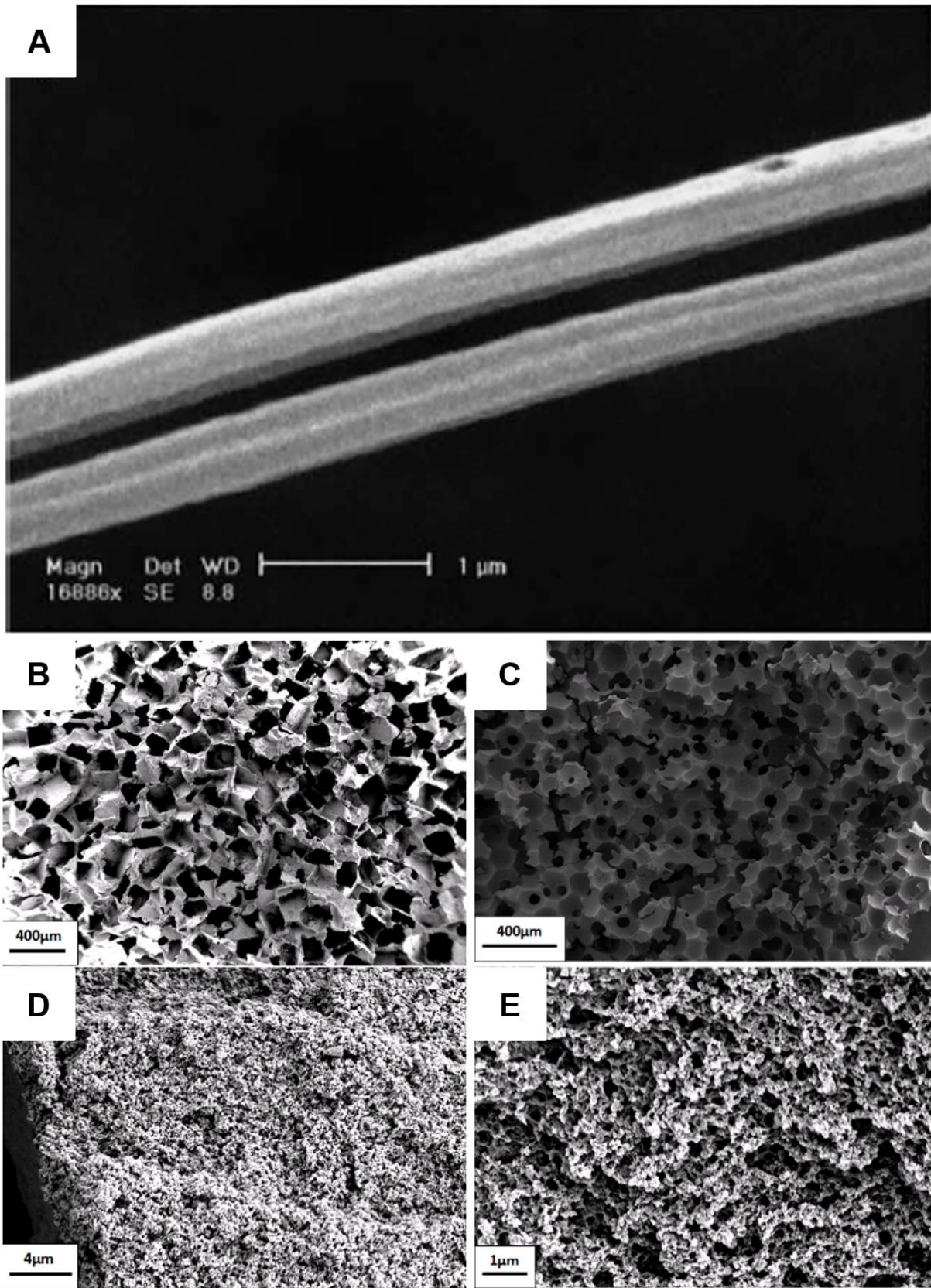
1 flow rate, the solvent volatility and polarity, the polymer solution viscosity and conductivity,
2 *etc.* Therefore, choosing appropriate (co)solvents and electrospinning parameters are crucial
3 to finely control the porous features of resulting polymeric materials (**Fig. 4A**) [92].
4

5 Alternatively, polymerization of High Internal Phase Emulsions (HIPEs) is a
6 technique of choice to prepare biporous polymeric frameworks [93, 94]. Such materials were
7 first designed by Barby and Haq from Unilever in the early 1980's [95]. In this patent, the
8 authors reported on the preparation of a biporous polymer network obtained after the
9 polymerization of a high internal phase emulsion, the porous polymer being subsequently
10 called polyHIPE. In such polyHIPE-based scaffolds, the higher porosity level arises from
11 drops of the discontinuous phase of the emulsion, while the lower one originates from the
12 interconnections between adjacent pores. PolyHIPEs can be prepared from water-in-oil (w/o)
13 [96], oil-in-water (o/w) [97] emulsions or from emulsified biphasic systems constituted by
14 two immiscible liquids [98] in the presence of surfactants that help to the emulsion
15 stabilization. Due to monomers and cross-linkers remaining in the external continuous phase,
16 w/o emulsions are appropriate to yield hydrophobic polymers such as styrenic polyHIPEs [99]
17 while o/w emulsions are suitable for the production of more hydrophilic polymers (**Fig. 4B**)
18 [97].
19



1
2 **Fig. 4.** Examples of biporous polymeric materials observed by SEM. (A) Biporous polymeric
3 material generated by a combination of electrospinning and particle leaching. [92], Copyright
4 2001 (Reproduced with permission from Wiley-VCH publishers). (B) Biporous polymeric
5 material obtained via high internal phase emulsion. [100], Copyright 2007 (Reproduced with
6 permission from Elsevier Ltd.).

7



1
 2 **Fig. 5.** Examples of doubly porous materials obtained through the double porogen approach.
 3 (A) Porous polyacrylonitrile prepared *via* a combination of electrospinning and CaCO_3
 4 particle leaching. [101], Copyright 2013 (Reproduced with permission from Wiley-VCH

1 publishers). Biporous poly(hydroxyethyl methacrylate) frameworks obtained *via* a
2 combination of NaCl particle leaching concomitant to the use of a porogenic solvent (B), (D)
3 or *via* extraction of PMMA beads and a porogenic solvent (C), (E). [102], Copyright 2015.
4 Reproduced with permission from Springer.

5
6 Last but not least, the double porogen templating approach consists in using two
7 different types of porogenic agents, *i.e.* one for the generation of pores within the micrometer
8 range and the other one to obtain pores within the nanometer range. For instance, the use of
9 electrospinning and particle leaching [101] (**Fig. 5A**) allowed for the preparation of materials
10 with a macroporosity generated by the fibers organization and a nanoporosity revealed by
11 calcium carbonate particle leaching using 1, 3, and 5% v/v of HCl aqueous solution,
12 increasing the specific surface area of the porous scaffolds. Another interesting approach
13 using two different porogens was described by Ly *et al.* Poly(HEMA-*co*-EGDMA) monoliths
14 were synthesized using macroporogenic agents consisting of fused PMMA beads [102] or
15 NaCl particles [102-106] and different porogenic solvents (**Fig. 5B,C**) [103]. The fused
16 macroporogens allow for the pores generated after particle leaching to be interconnected,
17 while the porogenic solvent gives rise to a lower porosity level, thus enhancing the specific
18 surface area of the resulting doubly porous materials. Different experimental conditions such
19 as the particle sintering conditions (Spark Plasma Sintering *vs.* vacuum oven), the particle
20 morphology (spherical *vs.* cubic) as well as the porogenic solvent nature were carefully
21 investigated. Such studies have led to optimized materials on which were immobilized gold
22 nanoparticles, thus leading to porous hybrid materials meant for heterogeneous supported
23 catalysis [105, 106].

24

1 2.5 **Characterization techniques of porous materials**

2 Different techniques have been so far developed for the fine characterization of porous
3 materials. In this way, critical information, including pore size, pore size distribution, pore
4 connectivity (open *vs.* closed, *i.e.* presence or absence of interconnections between adjacent
5 pores), and specific surface area, can be accurately determined using complementary physico-
6 chemical techniques in the laboratory.

7 Two different techniques are mainly used to determine the pore size of porous
8 polymeric materials. Such techniques rely on the type of porous materials under investigation.
9 Mercury intrusion porosimetry (also shortened as MIP, **Table 4**) is a specific technique
10 consisting in intruding a non-wetting liquid, *i.e.* mercury, into a porous sample placed within
11 a penetrometer. Upon applying an increasing pressure, mercury is forced to intrude into the
12 pores of the material [107]. Mercury does not wet materials, and so it will not penetrate pores
13 by capillary action, excepted if it is forced to do so by applying the said pressure. The pore
14 size can then be determined by correlating the pressure required for mercury intrusion into the
15 pores to the pore size *via* the Washburn equation (**Equation 1**) [108]:

$$16 \qquad P = \frac{-4\gamma \cos \theta}{D} \qquad (1)$$

17 where P is the pressure applied for the mercury intrusion, γ is the mercury surface tension, θ is
18 the contact angle between the mercury and the pore wall, and D stands for the diameter of the
19 pore being intruded.

20 It is noteworthy that the pores are supposed to be cylindrical in this equation, while
21 most of the real porosity is not. As said before, for MIP analyses, the porosimeter apply a
22 pressure to force mercury intruding the pores, and the Washburn equation allows for
23 determining the pore diameter [109]. Applying an increasing pressure indeed pushes known
24 amounts of mercury into the porosity of the material, and it thus allows for determining the
25 pore volume for a precise pore size. Additionally, knowing the distribution of the pore volume

1 with respect to its pore size provides the pore size distribution [110]. However, this technique
2 has some limitations especially regarding pore sizes in the nanometer range.

3 For materials exhibiting pore sizes that range from 2 to 300 nm, gas sorption is much
4 more appropriate, especially for accuracy reasons [111]. Gas sorption measurements can use
5 different gases: mostly N₂ [112] is used, but CO₂ [113] or Kr [114] can also be employed at a
6 precise temperature to obtain isotherms. Gas sorption porosimetry is now routinely used to
7 determine the specific surface area of porous materials, using the Brunauer-Emmett-Teller
8 (BET) method [115], whose equation is given below (**Equation 2**):

$$9 \quad \frac{P}{n^a(P_0-P)} = \frac{1}{n_m^a C} + \frac{(C-1)}{n_m^a C} \times \frac{P}{P_0} \quad (2)$$

10 where n^a is the gas amount adsorbed at the relative pressure $\frac{P}{P_0}$, n_m^a is the monolayer capacity,
11 and C is a constant, which is function of the isotherm shape. According to this equation, a
12 linear relation exists between $\frac{P}{n^a(P_0-P)}$ and $\frac{P}{P_0}$ so it is possible to determine n_m^a , thus leading to
13 (**Equation 3**):

$$14 \quad A(BET) = n_m^a \times L \times a_m \quad (3)$$

15 where $A(BET)$ is the specific surface area, L the Avogadro constant, and a_m the average area
16 occupied by each adsorbed molecule in the complete monolayer (*i.e.* the molecular cross-
17 sectional area).

18 Gas sorption measurements can also give pore sizes for porous materials exhibiting a
19 porosity from 2 to 300 nm using the so-called Barrett-Joyner-Halenda (BJH) method (**Table**
20 **4**) [116]. Similarly to MIP, this calculation method leads to a pore size distribution, but it is
21 limited for materials exhibiting pores higher than 0.1 μm .

22 Alternatively, a less widespread characterization technique can be used for the
23 porosity characterization of mesoporous materials, namely thermoporometry (**Table 4**), based

1 on differential scanning calorimetry (DSC) [117]. This technique relies on the Gibbs-
2 Thomson equation (**Equation 4**) [113]:

$$3 \quad D_p = 2 \left(A + \frac{B}{T_m - T_{m0}} \right) \quad (4)$$

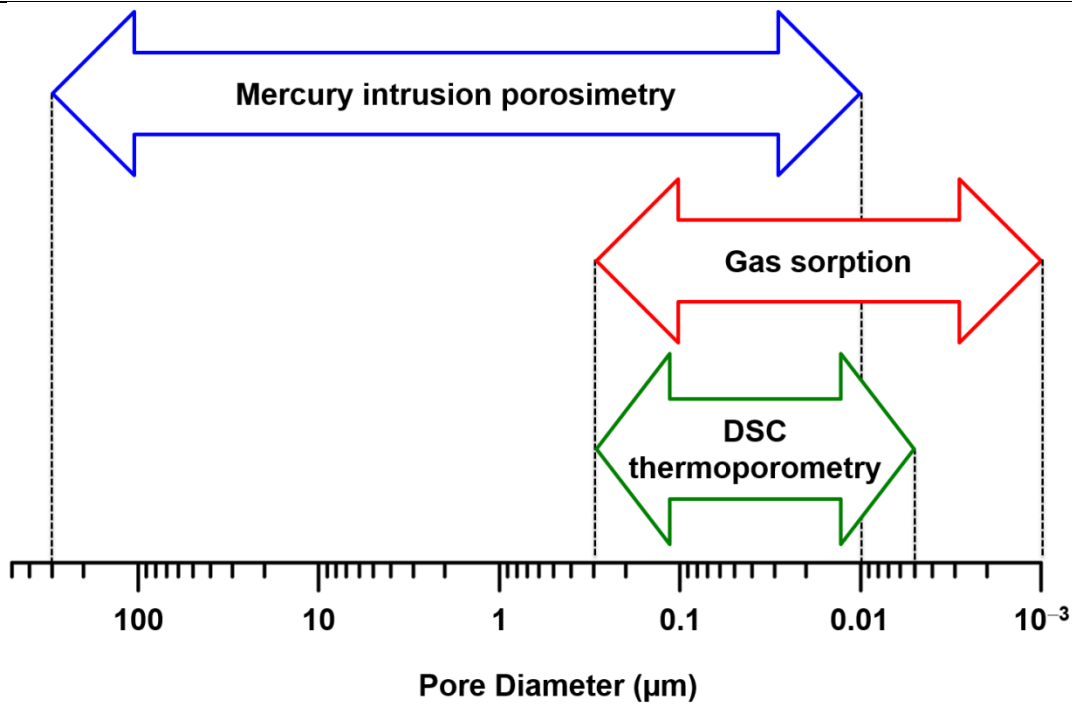
4 where D_p is the pore diameter, A and B are constants depending on saturating solvent, pore
5 geometry and measurements on cooling or heating, T_m and T_{m0} are the melting temperatures
6 of confined liquid and bulk liquid, respectively.

7 If a porous material is filled with a liquid, and then the latter is frozen, the melting
8 temperature T_m of the liquid will not be the same for that confined in the pores and that in the
9 bulk. T_m for the liquid in the pores will be lower, and the difference between T_m and the bulk
10 liquid melting temperature provides the pore diameter according to **Equation 4**. Besides,
11 comparing data from freezing and melting phenomena leads to precious information regarding
12 the pore shape. The limitation of this technique is due to its principle: if the pore size is too
13 high, the liquid confined into the pores will act as a bulk liquid. Therefore, the melting peak
14 of the confined liquid will be hidden into the profile of the bulk liquid melting peak and no
15 differences will be observable. However, DSC-based thermoporometry has been proved to be
16 effective using various solvents, like water [118], benzene [118], cyclohexane [119] or
17 acetonitrile [120] that are commonly used solvents. Another variation of the technique relies
18 on the use of nuclear magnetic resonance (NMR) [121].

19

1 **Table 4.** Common techniques used for the characterization of pore diameter in porous
 2 polymers and their characteristics.

Technique	Pore diameter range	Principle
Mercury Intrusion Porosimetry (MIP)	$\approx 300 \mu\text{m} - \approx 10 \text{ nm}$	Washburn equation
Gas sorption	$300 \text{ nm} - < 2 \text{ nm}$	Barrett-Joyner-Halenda (BJH) theory
DSC thermoporometry	$300 \text{ nm} - 5 \text{ nm}$	Gibbs-Thomson equation



3
 4 Finally, pycnometry can be used to determine an “apparent density” (more precisely a
 5 volume) of a porous solid, which is defined as the ratio between its mass and the total volume
 6 enclosed by an envelope of fluid. Pycnometry mostly uses gases, such as helium (He), but it
 7 can also be achieved with liquids, such as water or xylene. A typical pycnometer consists of
 8 two sealed chambers connected between them by a valve. The first chamber is used as a
 9 reference and the second one holds the sample. The sample chamber is filled with the fluid,
 10 while the other one is still under vacuum. Then, the valve is opened and the fluid is allowed to
 11 expand into the second chamber at a precise temperature while the pressure is measured, thus
 12 giving the volume of the sample V_S , *i.e.* the open porosity volume using the Boyle-Mariotte
 13 law (**Equation 5**) [122]:

1
$$V_S = V_C - \frac{V_r}{1 - \frac{P_1}{P_2}} \quad (5)$$

2 where V_C is the volume of the empty sample chamber, V_r is the volume of the second
3 chamber, P_1 is the first pressure in the sample chamber and P_2 is the pressure after expansion
4 into the combined volume of the chambers.

5 It is important to notice that pycnometry gives the volume of the open porosity. In the
6 case of a closed porosity in the sample, the density will be an effective one. To give access to
7 the closed porosity, two measurements are required: one with a porous system and another
8 with a bulk system. The comparison between both gives access to the volume of the closed
9 porosity [123]. This method has been extended to other porous polymeric systems to enable
10 the characterization of polymer gels for instance.

11

12 **3 Application of metallic nanoparticle immobilized on porous polymers as supported** 13 **catalysts**

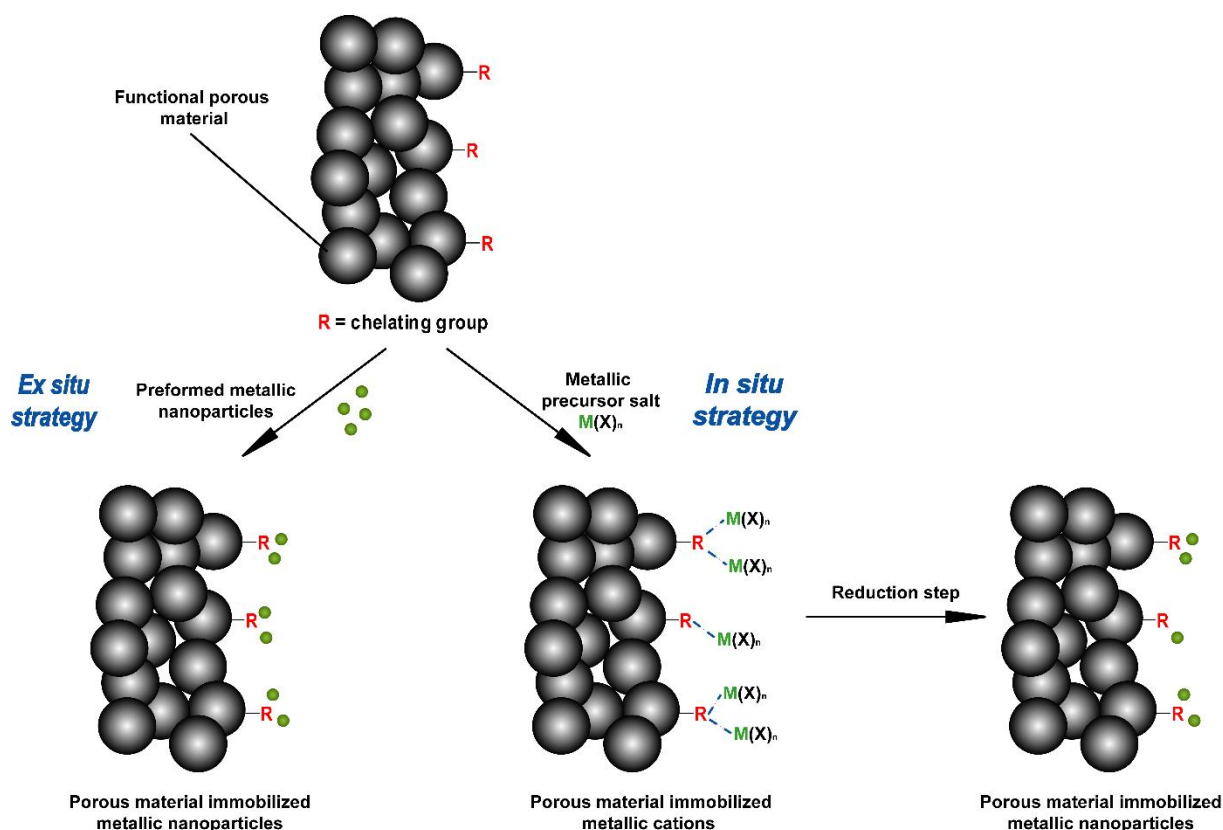
14 **3.1 Key features of nanoparticles**

15 Nanoparticles have been widely used as catalysts in the past decade, as they offer large
16 surface area and consequently enhanced catalytic activity. Well-documented reviews
17 discussing both synthesis and catalysis aspects can be found in the literature [124, 125] and, in
18 most cases, these reviews focused on a sole metal type. The reader is kindly referred to the
19 reviews by Takale *et al.* [126] or Daniel & Astruc [127] for critical discussion about gold
20 nanoparticles (Au NPs) and their catalytic uses, while Gawande *et al.* [128] and Ranu *et al.*
21 [129] focused on copper nanoparticles (Cu NPs). Chen & Holt-Hindle [130] and Astruc [131]
22 detailed platinum (Pt NPs), and palladium (Pd NPs) nanoparticles, respectively. Herein, we
23 purposely restricted the discussion to the cases of metal NPs supported on organic porous
24 polymers for catalysis in organic chemistry. Although supported catalysts have been much
25 less discussed, reviews present in the literature focused mainly on inorganic materials as

1 supports [129]. More specifically, one may cite the comprehensive survey by Corma and
2 Garcia [130] who exclusively summarized recent trends in nanogold supported onto inorganic
3 supports as catalysts for organic synthesis as well as that from Campelo and coworkers [131]
4 describing the synthesis and applications of nanoparticles of various metals.

5 Regarding the immobilization of nanoparticles onto solid supports, two main ways
6 have been reported to date in the literature, hereafter referred to as *ex-situ* and *in-situ* ways
7 (**Fig. 6**). It is crucial to mention that in order to achieve robust surface anchoring of metal
8 nanoparticles (MNPs), the supports may preferably bear accessible chemical moieties able to
9 induce specific interactions with the metal in its ionic or reduced forms. Amines, thiols,
10 cyanos, and carboxylic acids are representative examples ensuring strong interactions with
11 metals, such as gold, copper, palladium. In some cases, the interactions can occur between the
12 chemical units attached on solid surface and the stabilizing agent decorating the NP surface.
13 Porous polymers with chelating ability can be easily designed using monomers incorporating
14 functional side groups that may act as either chelation sites (for example 2-
15 (dimethylamino)ethyl methacrylate) or reactive sites for post-polymerization
16 functionalization. In the latter case, one may cite GMA, 4-VBC, NAS, or GCMA.

17 The *ex-situ* way requires the synthesis of the NPs prior to their immobilization onto
18 the pore surface. Well-established methods were typically applied for the synthesis of metal
19 colloids. In a further step, the NPs are immobilized onto the solid supports. A major
20 advantage of the *ex-situ* approach is that it offers the possibility to use commercially available
21 nanoparticles. Although it makes easier the whole synthesis process and provides fine control
22 over the size distribution and colloidal stability of the NPs, it may be restrictive in terms of
23 available size and shape.



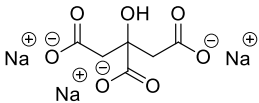
1
 2 **Fig. 6.** Scheme representing the two main ways, namely *ex situ* and *in situ* ways, for the
 3 immobilization of nanoparticles onto a porous support.
 4

5 In contrast, the *in-situ* way implies the generation of the NPs in presence of the solid
 6 supports and is thus a deposition precipitation process [132]. First, the support is immersed
 7 into a solution containing the salt of the metal of interest for impregnation purpose. Then, the
 8 metal is reduced to its zero state through a reduction step. Several reducing agents are
 9 routinely used in organic synthesis (**Table 5**) and can be also envisaged for metal reduction,
 10 like NaBH_4 [133, 134], citrates [135, 136] (in the so-called Turkevitch process), hydrazine
 11 [137] or even H_2 [138, 139]. The choice of the reducing agent will depend on the size and
 12 shape desired for the NPs and is crucial to achieve controlled synthesis. Indeed, depending on
 13 the metal – reducing agent pair, various levels of control on the shape, size and surface
 14 distribution will be obtained. Other important parameters are the strength of the interaction

1 between metal ions and the chemical groups at the surface of the support as well as the
2 reducing agent/salt precursor ratio.

3

4 **Table 5.** Examples of common reducing agents used for the preparation of nanoparticles.
5 Typical conditions for reduction are also provided.

Reducing agent	Formula	Conditions	References
Sodium borohydride	NaBH_4	Aqueous solution, r.t.	[133, 134]
Sodium Citrate		Aqueous solution, heat (reflux)	[135, 136]
Dihydrogen	H_2	Heat	[138, 139]
Hydrazine	$\text{H}_2\text{N-NH}_2$	Aqueous solution, heat or ultrasound	[137, 140]

6

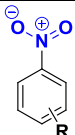
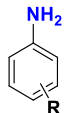
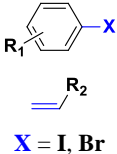
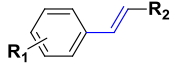
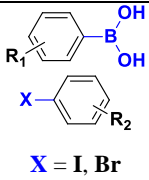
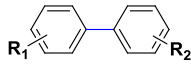
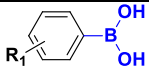
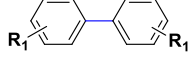
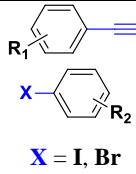
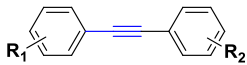
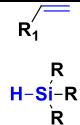
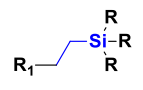
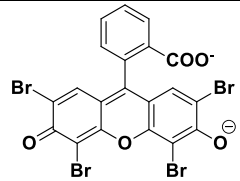
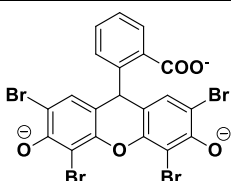
7 Although easy to implement, successful surface nanostructuring of porous polymers
8 with nanoparticles implies that the NPs are strongly anchored so that leaching phenomenon
9 does not occur. Indeed, the latter is detrimental to product purity as the presence of metal,
10 even at the trace levels, may induce toxicity to human beings. As such, the selection of the
11 chelating moiety is highly important and must be rationalized with respect to the nature of the
12 metal and stabilizing agents. Generally speaking, the stronger the interaction between the
13 support and the catalyst, the lower the possibility of leaching. One should of course keep in
14 mind that the conditions for the immobilization of the NPs may differ significantly from the
15 conditions for the catalysis applications. Changes such as solvent, pH and temperature may
16 affect the strength of the chelation. Finally, the supported catalyst may be in contact with a
17 variety of chemicals in the course of the catalytic cycles that may pollute the catalyst surface
18 and eventually affect the turnover number and frequency. Thus, regeneration is usually
19 required after several catalytic cycles.

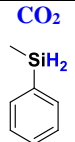
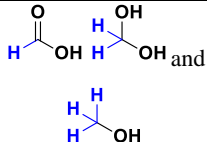
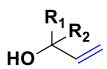
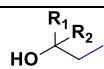
20

1 3.2 Nanoparticles supported by macroporous polymers

2 Supported catalysts have not been widely described in the literature and this is
 3 particularly true in the case of porous polymer-based supports. Herein, we purposely opted for
 4 a discussion on the basis of the type of polymeric support rather than the type of the catalyzed
 5 reaction or nature of the metal NP (**Table 6**).

6
 7 **Table 6.** Example of catalyzed reactions performed using metal nanoparticles supported on
 8 polymers.

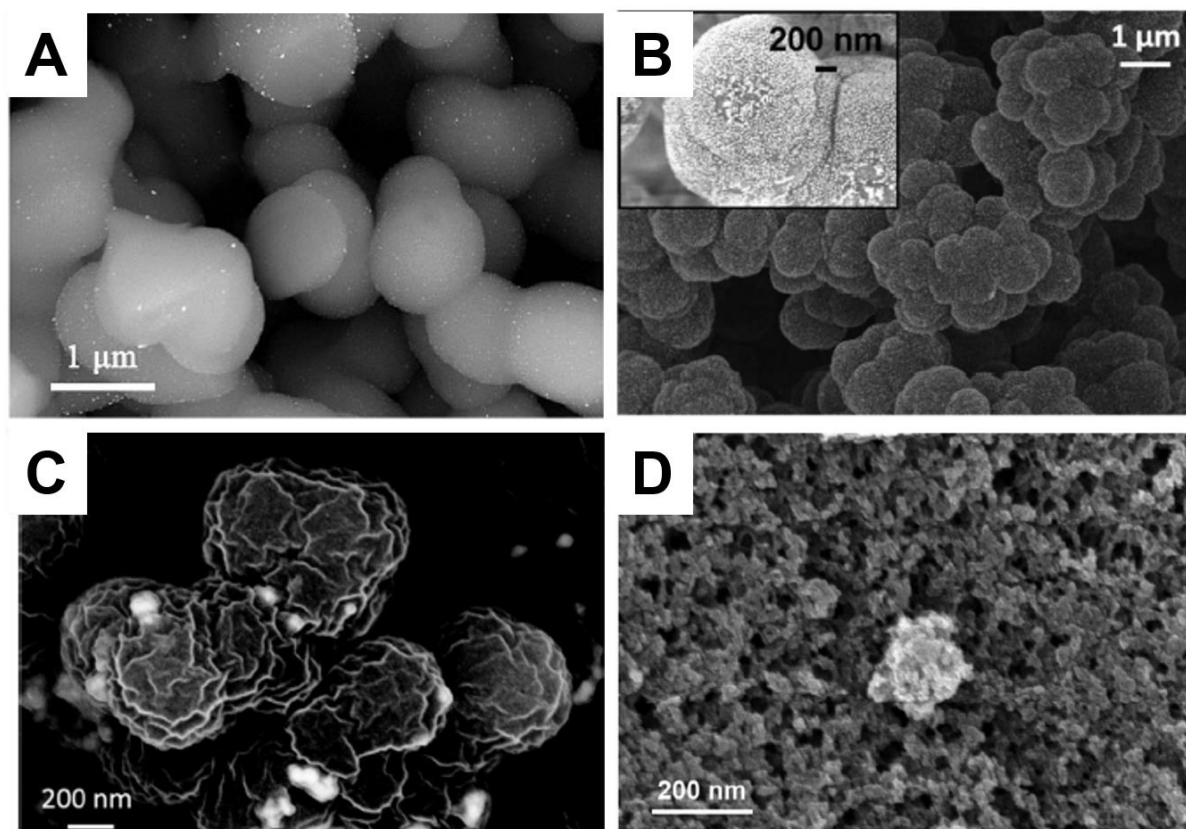
Name of the reaction	Reactant(s)	General conditions	Catalyst	Product(s)	References
Nitroarenes reduction		H ₂ O, NaBH ₄ , r.t.	Au, Ag, Cu, Pt, Pd		[31, 63, 66, 105, 106, 140-148]
Mizoroki-Heck coupling		DMF, Base, ≈ 100 °C	Pd		[149-151]
Suzuki-Miyaura coupling		Ethanol or DMF, Base, ≈ 100 °C	Pd		[145, 150- 157]
Boronic homocoupling		Ethanol, Base, ≈ 65 °C	Au		[63]
Sonogashira coupling		H ₂ O and THF, Base, ≈ 50 °C	Pd		[151, 157]
Hydrosilylation		<i>n</i> -hexane, 45 °C	Pt		[158]
Eosin Y reduction		H ₂ O, NaBH ₄ , r.t.	Au		[100, 159]
Reduction of hexacyanoferrate(III)	Fe(CN)₆³⁻	H ₂ O, NaBH ₄ or thiosulfate, r.t.	Au or Pd/Pt	Fe(CN)₆⁴⁻	[20, 160]

Carbon dioxide conversion		DMSO, r.t.	Pt		[161]
Hydrogenation of alcohol	 <p>R₁ = H or CH₃ R₂ = H or alkane group</p>	THF, H ₂ pressure, r.t.	Pd	 <p>R₁ = H or CH₃ R₂ = H or alkane group</p>	[162, 163]
Reduction of hexavalent chrome	Cr^{VII}	H ₂ O, formic acid, 50 °C	Au, Pd	Cr^{III}	[140, 164]
Reduction of U ^{VII}	U^{VI}	H ₂ O, formic acid, 50 °C	Pd	U^{IV}	[140]

1
2 As discussed above, macroporous polymers are essentially generated using a solvent as a
3 porogen [16]. Using such a process, many examples focused on the synthesis of monolithic
4 polymers within microchannels. The as-generated monolithic-based microsystems can be
5 used after immobilization of metal nanoparticles either as sorbents for solid phase extraction
6 or separation purposes or as microreactors for flow through catalysis. One may briefly
7 mention papers from teams of Svec, Buchmeiser, Connolly or Carbonnier who have extended
8 the concept of metal nanoparticles decorating monoliths as chromatographic microcolumns
9 to supported catalysts in continuous flow microreactors [18, 165-167]. In their pioneering
10 work, Nikbin, Ladlow & Ley described in 2007 the synthesis of a vinylbenzyl chloride-based
11 column and its subsequent functionalization with triethylamine to generate ammonium groups
12 at the pore surface [149]. The porous features of the obtained monolithic column were
13 investigated both by MIP and BET techniques, showing a median pore size of 3.15 μm and a
14 surface area of about 5 $\text{m}^2\cdot\text{g}^{-1}$. The available surface groups were used to immobilize Pd NPs
15 onto the pore surface through a deposition precipitation process. First, the porous polymer
16 was flushed with an aqueous solution of Na_2PdCl_4 (20 mM) followed by *in-situ* reduction of
17 the surface immobilized Pd ions with sodium borohydride. The reactor was used for the
18 Mizoroki-Heck reaction of different iodobenzyls with styrene and acrylate derivatives

1 providing high yields above 80% (**Table 7**). The authors conclusively demonstrated that flow-
2 through processes were superior to batch reaction, notably because of the possibility of
3 processes automation.

4 The Buchmeiser group worked on the preparation of porous materials into chromatographic
5 columns based on Ring Opening Metathesis Polymerization (ROMP), and suggested several
6 potential applications. Restricting the discussion to supported catalysis, they developed
7 monoliths bearing platinum (**Fig. 7A**) or palladium-based nanoparticles, obtained through the
8 *in-situ* reduction of the corresponding salts, and proved their efficiency for several catalytic
9 reactions like hydrosilylation [158] and carbon dioxide conversion [161] or Mizoroki-Heck
10 [150], Suzuki-Miyaura [150] (**Table 7**) and Sonogashira [157] (**Table 7**). Of particular
11 interest, the authors reported high TurnOver Numbers (TONs, representing the number of
12 moles of reactants that a mole of catalyst can convert before decrease in the catalyst activity).
13 TONs values higher than 600 000 were reported for the hydrosilylation reaction.



1
2 **Fig. 7.** Examples of macroporous polymeric materials bearing metallic nanoparticles. (A) *in-*
3 *situ* generated Pt NPs onto a ROMP-generated-matrix capillary. [158], Copyright 2012
4 (Reproduced with permission from the Royal Society of Chemistry). (B) *ex-situ* generated Au
5 NPs onto a NAS-matrix capillary. [146], Copyright 2017 (Reproduced with permission from
6 the Royal Society of Chemistry). (C) *ex-situ* generated Cu NPs onto a NAS-matrix capillary.
7 [31], Copyright 2015 (Reproduced with permission from Elsevier Ltd.). (D) *in-situ* generated
8 Au NPs onto a DSDMA bulk monolith. [159], Copyright 2017 (Reproduced with permission
9 from Elsevier Ltd.).

10
11 Connolly's team used glycidyl methacrylate- and vinyl azlactone-based monoliths to anchor
12 as-prepared gold nanoparticles [160] as well as bimetallic platinum/palladium nanoflowers
13 [20]. In both cases, the NPs were synthesized *ex-situ* according to literature protocols, and
14 then flushed directly into polymer-filled capillaries or pipette-tips. Amine moieties were
15 grafted onto the polymeric surface using ethylenediamine and were used to anchor both types
16 of nanoparticles. The as-designed supported catalysts were used to reduce a ferric complex,

1 hexacyanoferrate $\text{Fe}(\text{CN})_6^{3-}$, into $\text{Fe}(\text{CN})_6^{4-}$ using NaBH_4 as a co-reagent. BET measurements
 2 performed on the GMA- and vinyl azlactone-based monoliths bearing gold and bimetallic
 3 nanoflowers showed a significant decrease in the surface area of the materials before and after
 4 adsorption of preformed nanoobjects from 40 to $12 \text{ m}^2 \cdot \text{g}^{-1}$. The authors explained these rather
 5 surprising results by a potential clogging of the porosity by the adsorbed 20-nm sized
 6 nanoflowers.

7

8 **Table 7.** Examples of C-C coupling reactions achieved using polymer-supported metal
 9 nanoparticles. The reactions conditions and yields are also presented.

Reaction	Experimental conditions	Supported metal catalyst	Yield
Suzuki-Miyaura coupling	THF/ H_2O (50/50 % v/v), 1.5 eq. <i>t</i> -BuOK, 1 eq. NBu_4Br , 50 °C, 24 h	Pd	54 % to 99 % (various haloarenes tested) TONs: 34 400 to 63 000
	EtOH; 2.5 eq. <i>t</i> -BuOK, 50 °C, 24 h	Pd	96 %
Mizoroki-Heck coupling	Dioxane, 0.6 mmol benzonitrile, 80-130 °C, 72 h	Pd	77 % to 100 %
	DMF, 0.3 mmol trimethylamine, 130 °C, flowrate: $0.05 \text{ mL} \cdot \text{min}^{-1}$	Pd	<50 % to 87 % (various pairs of reactants)
Sonogashira coupling	5mmol trimethylamine, 90 °C, MW 300 W	Pd	Methyl acrylate <20 % to 83 % for $t = 1 \text{ min}$ 50 % to >99 % for $t = 5 \text{ min}$ Styrene 35 % to 85 % for $t = 10 \text{ min}$
	THF/ H_2O (50/50 % v/v), 1.5 eq. <i>t</i> -BuOK, 1 eq. NBu_4Br , 50 °C, 24 h	Pd	2 % to 95 % (various haloarenes tested) TONs: 90 to 4130
Sonogashira coupling	2 mmol DABCO, 130 °C, MW 300 W, 2 min	Pd	>90 % to >99 %

References	[150]	[152]	[156]	[149]	[151]	[157]	[157]
------------	-------	-------	-------	-------	-------	-------	-------

1
2 Carbonnier's group contributed a lot to the field of flow-through supported catalysis by
3 developing a series of chemically modified monolithic supports based on NAS. The generic
4 monolith was initially synthesized within microsized channels and further chemically
5 modified by taking advantage of the reactive of the *N*-hydroxysuccinimide moieties towards
6 nucleophilic species. Such in-capillary monoliths displayed a pore size of 2.25 μm by MIP, a
7 surface area lower than $10 \text{ m}^2.\text{g}^{-1}$ but a large porous volume of *ca.* $1.5 \text{ cm}^3.\text{g}^{-1}$ [25]. One of the
8 first examples described the preparation of diacid-decorated porous monolith [31]. Such
9 carboxylic acids were used to anchor copper nanoparticles using two immobilization
10 processes. On the one hand, commercially available copper nanoparticles (with mean
11 diameter in the range 40–60 nm) were percolated into the monolithic structure and the
12 microreactor used directly after a rinsing step. On the other hand, Cu^{2+} ions were initially
13 immobilized onto the surface of the functionalized monolith. In a second step, an aqueous
14 NaBH_4 solution was injected in the monolith to generating the nanoparticles through
15 reduction. Both microreactors were used to catalyze hydride-mediated reduction of one
16 nitroarene, the *o*-nitrophenol. The best yield (68.5 % at a flow rate of $0.3 \mu\text{L}.\text{min}^{-1}$) was
17 obtained when preformed NPs were used while the *in-situ* approach led to slightly lower
18 yields (40 and 55 % for flow rates of 4 and $1.5 \mu\text{L}.\text{min}^{-1}$, respectively) (**Table 8**).

19 In another implementation, the NAS-based monolith was used as support for gold
20 nanoparticles. As described in the work of Khalil *et al.* [147], ethylenediamine was grafted on
21 the monolith surface. The resulting primary amines, in their protonated form, were used as
22 ligands to immobilize Au colloids. Both ways of nanoparticles immobilization, namely *in-situ*
23 and *ex-situ* pathways were investigated. In the former case, an aqueous solution of HAuCl_4

1 was percolated to immobilize Au³⁺ ions followed by reduction using an aqueous NaBH₄
2 solution. For the *ex-situ* way, commercially available Au NPs with a diameter of 20 nm and a
3 citrate stabilization layer were used. Interaction between the carboxylates of the citrates and
4 the ammonium form of the primary amines at the pore surface provided strong interfacial
5 interaction, leading to robust anchoring of the nanoparticles. The microreactors were used for
6 nitroarenes reduction, using *p*-nitroaniline, *o*-nitrophenol, *m*-nitrophenol and *p*-nitrophenol as
7 model molecules. Different parameters were investigated to optimize the reaction yields, like
8 the reactants concentration, the column length, the flow rate allowing for complete conversion
9 of the nitroarenes into the corresponding aromatic amines. Of particular interest, it was shown
10 that the *in-situ* approach provided higher reaction yields as compared to the *ex-situ* using the
11 same flow conditions.

12 An extension of this work was provided in the paper by Liu *et al.* [146] where NAS-based
13 monoliths were functionalized with amine moieties derived from histamine. Commercially
14 available Au NPs with different sizes 5 nm, 20 nm (**Fig. 7B**) and 100 nm were used. The
15 aggregation behavior of the NPs at the monolith surface as well as the coverage density were
16 found to depend on the chemical nature of the amine ligand and size of the nanoparticles.
17 While the higher diameters (100 and 20 nm) were the most homogeneously and densely
18 covered columns, difficulties were encountered with the 100 nm Au NPs in the filling and the
19 back pressure obtained from the capillary. The catalytic efficiency of these microreactors was
20 first established for *p*-nitrophenol and then extended to dinitro derivatives, namely 2,5-
21 dinitrophenol, 2,4-dinitroaniline, 2,6-dinitroaniline and 3,5-dinitroaniline. Interestingly, the
22 best results were obtained for the 20 nm nanoparticles, instead of the 5 nm ones, and for a
23 flowrate of 5 μL.min⁻¹ (**Table 8**).

1 **Table 8.** Examples of nitro compounds reactions achieved using polymer-supported metal
 2 nanoparticles. The reactions conditions and yields are also presented.

Experimental conditions	Metal catalyst	Yield	References
Acetonitrile/H ₂ O (70/30 % v/v), [NaBH ₄] = 1.2 × 10 ⁻¹ M	Cu	68.5 % (ex situ) at 0.3 μL.min ⁻¹ 40 % (in situ) at 4 μL.min ⁻¹ 55 % (in situ) at 1.5 μL.min ⁻¹	[31]
H ₂ O, [NaBH ₄] = 1.2 × 10 ⁻¹ M, flowrate: 2 μL.min ⁻¹	Pt	100 %	[141]
H ₂ O, [NaBH ₄] = 1.2 × 10 ⁻¹ M, flowrate: 5 μL.min ⁻¹	Au	100 % (various nitro and dinitro compounds)	[146]
H ₂ O; [NaBH ₄] = 2 × 10 ⁻² M, 25 min	Au	95.4 %	[143]
H ₂ O, [NaBH ₄] = 0.25 M, 30 min	Ag	100 %	[142]
H ₂ O, [NaBH ₄] = 6.67 mM, 16 min	Pd	100 %	[140]
H ₂ O, [NaBH ₄] = 1.2 × 10 ⁻¹ M	Au	Macroporous 27 % at t = 1 h Nanoporous 25 % at t = 1 h 71 % at t = 40 min Biporous 93 % at t = 1 h 83 % at t = 40 min	[105, 106]

3
 4 Moreover, Carbonnier's group developed a new monolithic matrix, based on glycerol
 5 carbonate methacrylate [141]. Such a carbonate ring can be easily converted into a urethane
 6 group when reacting with a suitably chosen amine-bearing molecule. A determination of the

1 pore size of these in-capillary monoliths was achieved using mercury intrusion porosimetry.
2 The authors found an average pore size centered around 2.2 μm but also another lower
3 porosity level in the 50 nm range that was not visible by SEM because of the detection limit
4 of the apparatus. Carboxylic acids were grafted at the surface *via* a two-step process and then
5 used to chelate platinum ions. NaBH_4 was used as a reducing agent for the generation of Pt
6 NPs directly onto the pore surface. The as-prepared supported catalyst was further used for
7 the total reduction of *p*-nitrophenol (**Table 8**).

8 Beside the design of porous materials for flow-through applications, Poupart *et al.* also
9 prepared bulk polymeric materials using the porogenic solvent approach. A dimethacrylate
10 monomer bearing a disulfide bridge, namely bis(2-methacryloyl)oxyethyl disulfide
11 (DSDMA), was used with the aim to eventually produce thiol-containing monoliths [159].
12 Such an approach was followed because of the difficulty to polymerize thiol-containing
13 monomers with the occurrence of chain transfer reactions. Herein, they used a protected thiol
14 in the form of disulfide. After polymerization with a dimethacrylate as a cross-linker and
15 using toluene as a porogenic agent, thiols were generated using D,L-dithiothreitol (DTT).
16 Several solvents were used as porogens (methanol, ethanol, a cyclohexanol/dodecanol
17 mixture as well as toluene). Mercury intrusion porosimetry was performed on all samples,
18 even after DTT-mediated cleavage of the disulfide bridge contained in the monoliths. Average
19 pore sizes of 6 and 0.5 μm were determined for methanol and ethanol, respectively. Similarly,
20 average pore sizes of 0.01 and 1 μm were obtained for the cyclohexanol/dodecanol mixture
21 and toluene, respectively. No significant variation of pore size or porosity ratio was found
22 upon selective cleavage of disulfide bridges. Gold ions were subsequently anchored to the
23 thiolated surface and further reduced using sodium borohydride to generate Au nanoparticles
24 (**Fig. 7C**). Although aggregation trends could be seen onto the SEM pictures, the as-prepared
25 bulk catalysts were used to reduce an organic dye, Eosin Y. Up to six consecutive catalytic

1 cycles were tested with an average yield of about 60 %, thus ascertaining the reusability of the
2 supported catalyst.

3

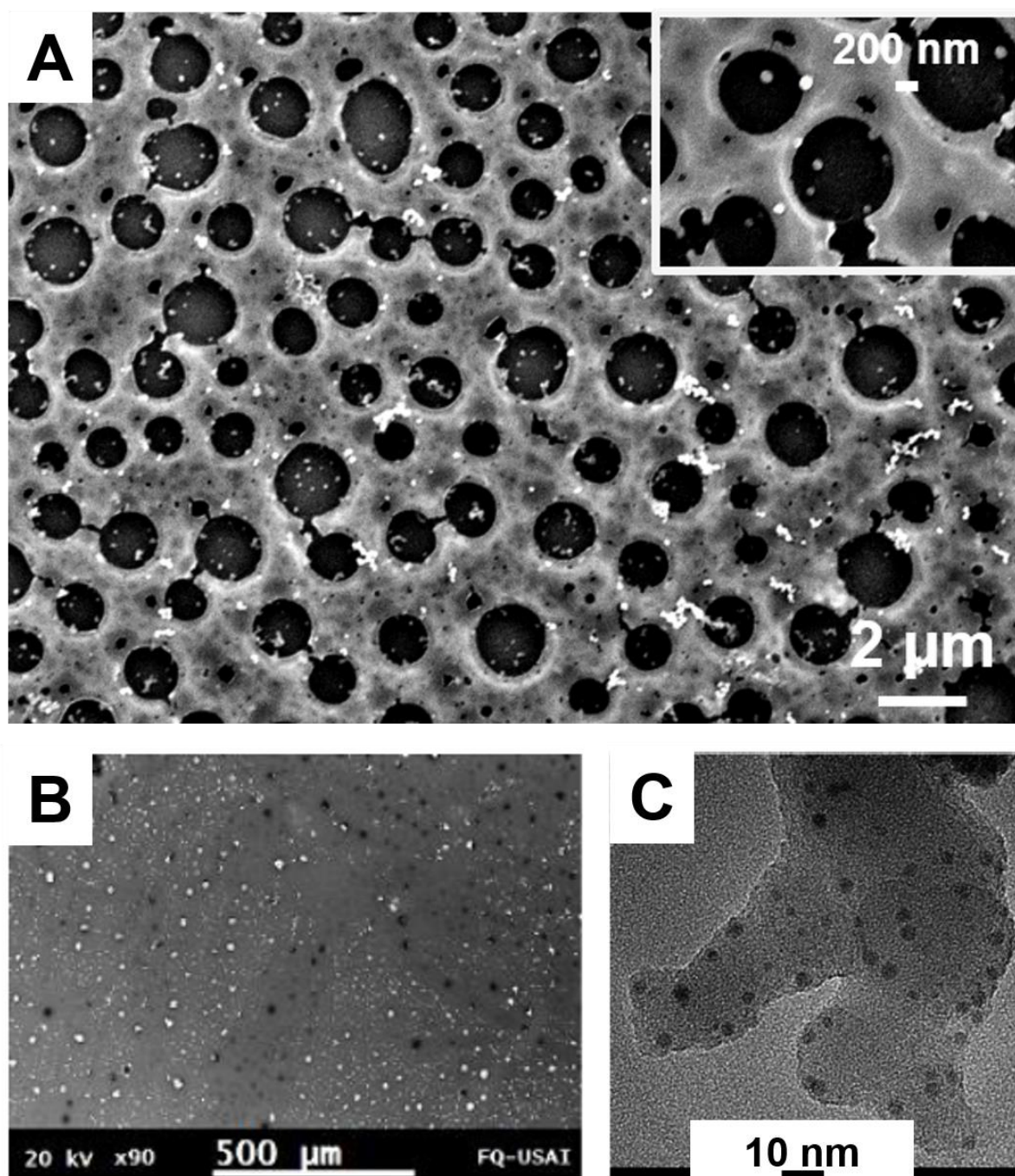
4 **3.3 Nanoparticles supported by nanoporous polymers**

5 As previously discussed, pore sizes of nanoporous materials are appealing for catalysis
6 applications, as they can provide a filtration phenomenon occurring simultaneously to the
7 catalytic activity. Few examples in the literature described the use of nanoporous polymers
8 arising from diblock copolymers. The first example of nanopore decoration with a metal was
9 reported by Ryu *et al.* [67] who generated gold nanorods at the interface of thiolated
10 polymers. Unfortunately, the authors did not mention any application. Recently, Grande's
11 group started to investigate how such pores could be decorated with nanoparticles and
12 considered the use of the resulting composite materials as supported catalysts.

13 In 2015, the synthesis of a diblock copolymer made of PS and PLA and bearing a disulfide
14 bridge junction between both blocks was first developed [66]. After the synthesis of the dual
15 initiator and both blocks by ATRP and ROP, an orientation step of the resulting functional
16 copolymer was implemented using a channel die process. Cleavage of the disulfide bridge
17 was achieved using triphenylphosphine (TPP), revealing the pores as well as the thiol
18 moieties at the pore interface. Au³⁺ ions were then immobilized and further reduced with
19 NaBH₄. The as-obtained porous polymer-supported gold nanoparticles were used as efficient
20 catalysts to reduce *p*-nitrophenol. Reaction yields of ≈ 70 % were calculated after 1 h of
21 reaction for five consecutive catalytic runs.

22 In another implementation, the same authors used an acetal junction between the two blocks
23 [63]. The dual initiator was synthesized *via* a two-step process, and after the polymerization
24 processes, orientation of the block copolymer structure was performed *via* solvent vapour
25 annealing of films casted onto Si wafers. The acetal link between both blocks could be easily

1 cleaved with trifluoroacetic acid and then, functionalized with amine molecules after
2 reductive amination reaction. Amine-decorated pores were covered with *in-situ* generated
3 gold nanoparticles (**Fig. 8A**). First, boronic homocoupling and nitroarene reduction were
4 considered separately. Finally, the two reactions were coupled in a cascade reaction process
5 involving 3-nitrobenzene boronic acid. After formation of the 3,3'-dinitrobiphenyl through
6 homocoupling reaction, the nitro moieties were successfully reduced using NaBH₄-mediated
7 reduction yielding 3,3'-diaminobiphenyl as a major product.



1
 2 **Fig. 8.** Examples of nanoporous polymeric materials bearing metallic nanoparticles. A) *in-situ*
 3 generated Au NPs onto a PS arising from diblock copolymers. [63], Copyright 2017
 4 (Reproduced with permission from the American Chemical Society). B) *in-situ* generated Au
 5 NPs within a cellulose membrane. [143], Copyright 2017 (Reproduced with permission from
 6 Wiley VCH). C) *in-situ* generated Pd NPs onto a microporous polyheptazine. [155],
 7 Copyright 2017 (Reproduced with permission from the American Chemical Society).
 8

1 Besides the use of diblock copolymers, several authors have implemented polymer-based
2 membrane materials exhibiting nanoporosity to design supported catalysts. Remigy and
3 Lahitte's group discussed the use of commercially available polyethersulfone membranes
4 with a pore size of 200 nm. The membranes were modified to anchor Pd NPs and further used
5 in several reactions, including nitrophenol reduction [144, 145], Suzuki-Miyaura cross
6 coupling [145, 152, 153] (**Table 7**) or hydrogenation of *trans*-4-phenyl-3-buten-2-one [163].
7 Interesting comparison was performed considering the use of these membranes in batch mode
8 and under flow-through conditions. The latter conditions proved to be superior providing
9 faster reactions. Indeed, while the reactions could be performed within a 10 s range in flow
10 conditions, the batch mode required 6 h for full conversion. Another interesting result was
11 that no byproducts were observed in the flow-through mode. This was assumedly assigned to
12 a lower kinetic of formation of the side product.

13 Other research groups focused on using membranes with embedded nanoparticles. One may
14 cite the work from Mora-Tamez *et al.* [143] who considered the use of Au NPs immobilized
15 within cellulose triacetate-based membranes. The originality of the approach lies in the
16 extraction of Au^(III) ions by the membranes and their simultaneous *in-situ* reduction with a
17 citrate solution (**Fig. 8B**). Such supports with embedded NPs were used for the reduction of *p*-
18 nitrophenol. The authors mentioned reaction yield as high as 95.4 % after 25 min of reaction
19 (**Table 8**). Membranes were also characterized using BET and nitrogen adsorption/desorption
20 isotherms. Specific surface area values ranging from 67 to 137 m².g⁻¹ and pore volume values
21 from 0.048 to 0.097 mL.g⁻¹ were found.

22 Likewise, Clark's group used biobased nanoporous polymers for catalysis purposes. Starch-
23 based porous supports were obtained by solvent exchange between water and ethanol, and
24 subsequently used to anchor palladium nanoparticles [151]. Palladium acetate was put in the
25 presence of the starch-based materials acting simultaneously as reducing agent and support

1 for the resulting nanoparticles, seemingly self-reducing the precursory metallic ions. Such
2 polymeric materials, characterized by N₂ physisorption, exhibited a specific surface area of
3 190 m².g⁻¹ and an average pore size of 8.2 nm through the BET equations (**Equation 2** and
4 **Equation 3**) as well as the BJH method, respectively. Mizoroki-Heck (**Table 7**), Sonogashira
5 (**Table 7**) and Suzuki-Miyaura reactions were performed under microwave irradiation using
6 the starch-supported Pd NPs. The microwave activation permitted to reduce the reaction time
7 as the reactions could be achieved in less than 10 min. In contrast, the authors provided a
8 comparison with other data published in the literature without the use of microwave and for
9 which the reaction times were in the range of 4-12 h. Although the authors concluded on the
10 superiority of the starch-based materials in terms of improved reaction yields, lower reaction
11 times, and renewability of the catalysts, a reliable comparison with traditional catalysts such
12 as Pd/C or silica-supported NPs is, to our point of view, very difficult because most of the
13 studies that the authors referred to did not mention the use of microwave activation.
14 Finally, microporous polymers (with pores below 2 nm) were used as catalytic supports.
15 Although most of examples in the literature mentioned the direct use of a polymer network as
16 the heterogeneous catalyst due to a specific site like a specific chemical moiety [168] or a
17 metallo-organic complex [169], some examples about polymer-supported nanoparticles can
18 also be found. Zhang *et al.* [154] designed a porous network *via* a direct Sonogashira coupling
19 of an aromatic trialkyne and 1,4-dibromobenzene. The as-obtained nanoporous polymer was
20 further characterized using N₂ sorption. First, BET measurements gave a specific surface area
21 of 421 m².g⁻¹ and a pore volume of 0.27 mL.g⁻¹. In this case, the pore size was not determined
22 using the BJH theory but was calculated by the nonlocal density functional theory (NLDFT),
23 a computational quantum mechanical modelling that allowed for highlighting the presence of
24 three populations of pores in such a material with sizes centered on 0.6, 1.3, and 3.1 nm. The
25 polymeric material was subsequently immersed into an acetone solution of Pd(OAc)₂. After

1 stirring at 90 °C, a Pd NPs-loaded polymer was obtained. Different Suzuki-Miyaura C-C
2 coupling reactions were performed using a large panel of halogenoarenes (iodo and bromo)
3 along with phenylboronic acid. High yields (> 85 %) and short reaction times (less than 4 h)
4 were obtained. Comparison with Pd/C catalysts suggested that such nano Pd-decorated
5 frameworks allowed for a threefold decrease of the reaction times (from 9 h for Pd/C to 3 h)
6 to reach similar reaction yields. Five catalytic cycles were performed and only a limited
7 reduction in catalytic activity was observed as expressed by the decrease of a few percent of
8 the reaction yields, while leaching effect was quantified to be less than 1 % for each cycle.

9 In their interesting work, Du *et al.* [155] prepared polymer networks through a nucleophilic
10 substitution of chlorines pending on the cyameluric chloride monomer by amines of
11 piperazine. The as-obtained heptazine framework was immersed into an acetone solution of
12 palladium acetate under reflux, allowing for the generation of the Pd NPs by self-reduction
13 (**Fig. 8c**). Similarly to the studies achieved by Zhang *et al.* about microporous polymeric
14 materials, the surface area of their porous heptazine framework was also determined through
15 BET measurements using nitrogen sorption. Surface area of 106 and 73 cm².g⁻¹ and pore
16 volume of 0.43 and 0.33 mL.g⁻¹ were found by the authors for the materials before and after
17 immobilization of Pd NPs, respectively. Such surface area values are rather unexpected; one
18 would indeed expect higher values for hybrid materials, likely due to the adsorption of
19 metallic nanoparticles at the pore surface of these polymeric frameworks. Pore size
20 distribution was also found in the 2-8 nm range. With such hybrid catalysts, Suzuki-Miyaura
21 couplings were performed using different pairs of bromoarenes derivatives and phenylboronic
22 acids. Yields above 80 % of conversion were obtained except for the 2-bromonaphthalene
23 along with the arylboronic acid as well as for the 4-nitrobenzene boronic acid along with
24 bromobenzene, for which yields remained below 40 %. A tentative explanation for the
25 obtained yields was provided by the authors based on the large steric hindrance of 2-

1 bromonaphtalene as well as the poor solubility of 4-nitrobenzene boronic acid. Here again,
2 five catalytic runs were performed consecutively showing a limited decrease of the catalytic
3 activity and ICP measurements performed before and after the five cycles showed negligible
4 leaching phenomena.

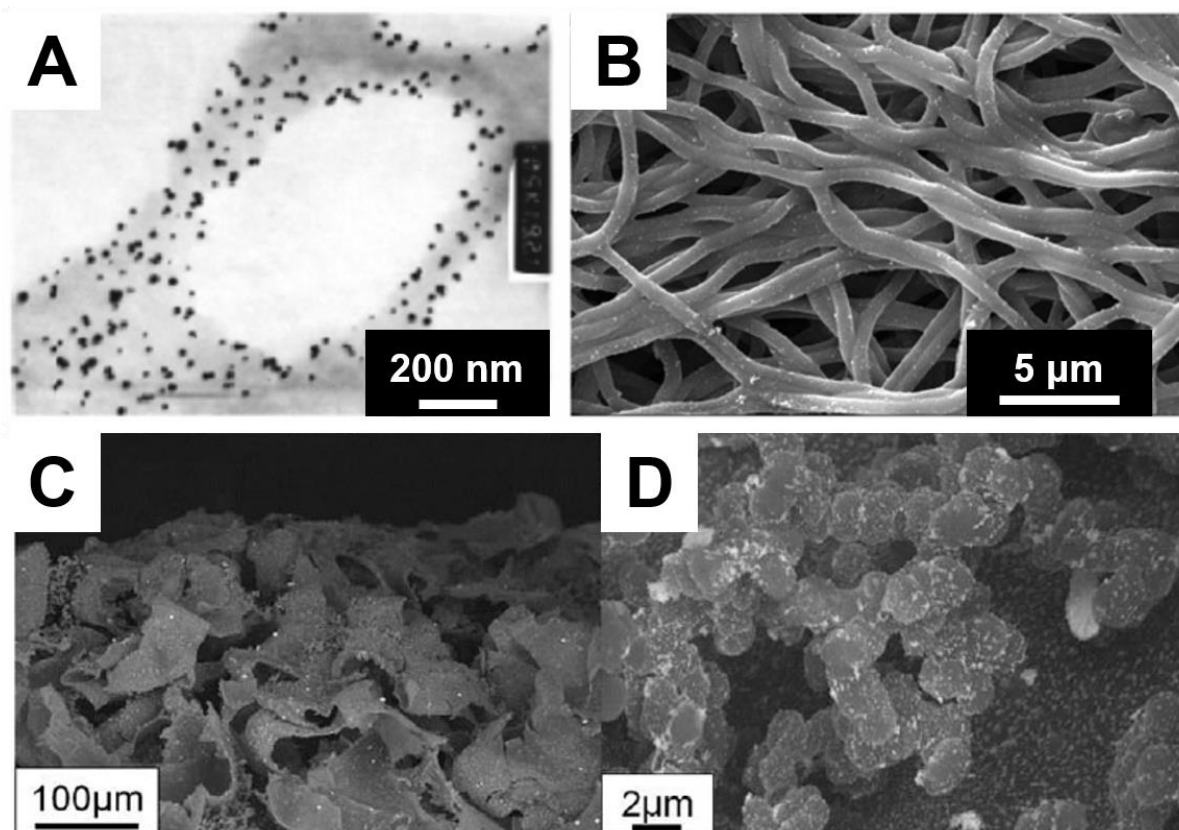
5

6 **3.4 Nanoparticles supported by biporous polymers**

7 Macroporous and nanoporous polymers are very different systems in terms of
8 permeability, porosity, surface area which are key features for catalysis applications.
9 Macroporous polymers possess large pores providing enhanced permeability for the liquid to
10 penetrate into the pores but a poor specific surface area. In contrast, nanoporous frameworks
11 afford a larger specific surface area, while a lower accessibility to the pores. A high
12 permeability may favor better accessibility of the reactants to the catalysts, while a large
13 specific surface area should allow for higher density of metal nanoparticles on the support
14 surface. If considered simultaneously, these two criteria may provide more efficient catalytic
15 processes. Based on this simple consideration, biporous materials containing both macropores
16 and nanopores may appear as attractive candidates for nanocatalyst supports.

17 An easy way of making biporous materials relies on the fabrication of polyHIPEs. One of the
18 pioneering groups in the field of polyHIPE preparation and use as catalysts is Deleuze's. In
19 2005, they described polystyrene- [162] and poly(vinylbenzyl chloride)-based [156]
20 polyHIPEs as supports for *in-situ* generated Pd NPs (**Fig. 9A**). Both styrene and VBC-based
21 polymeric supports showed a specific surface area of $902 \text{ m}^2 \cdot \text{g}^{-1}$ as determined by BET, while
22 pore size distribution in the 10-80 nm range was induced by a porogenic solvent added to the
23 HIPE polymerization feed. The hybrid supports were used for the hydrogenation of an alkene,
24 *i.e.* allyl alcohol, and for Suzuki-Miyaura cross-coupling reactions (**Table 7**). The authors
25 reported reaction times of 1 h and 70 h for near-completion hydrogenation and coupling

1 reactions, respectively. The authors discussed their results with respect to other published
2 results obtained with catalysts such as Pd/C using the prepared supported catalysts in powder
3 forms. Polystyrene based polyHIPEs were also used by the same group as supports for gold
4 nanoparticles [100]. In this case, HAuCl_4 ions solutions were simply deposited and the PS
5 induced self-reduction. Supported Au NPs were then used for the reduction of a dye, Eosin Y,
6 and the reaction was repeated three times. Near-completion reactions were achieved within
7 one hour and under mild conditions ($25\text{ }^\circ\text{C}$). Pores in the $200\text{-}291\text{ }\mu\text{m}$ range, were found for
8 such monoliths depending on the samples, while a porosity ratio of 82% was found by MIP.



10 **Fig. 9.** Examples of biporous polymeric materials bearing metallic nanoparticles. (A) *in-situ*
11 generated Pd NPs onto a PS polyHIPE. [162], Copyright 2005 (Reproduced with permission
12 from the American Chemical Society). (B) *in-situ* generated Ag NPs onto poly(acrylic acid)
13 fibers. [142], Copyright 2012 (Reproduced with permission from the Royal Society of
14 Chemistry). (C), (D) *in-situ* generated Au NPs onto a biporous poly(HEMA-*co*-EGDMA)
15 bulk monolith. [104], Copyright 2016 (Reproduced with permission from Wiley VCH).

16

1 Another way to design nanostructured catalysts relies on the use of electrospun materials. The
2 as-obtained fibers possess several interesting properties for catalytic applications, such as a
3 large surface to volume ratio and superior mechanical properties. Therefore, they are also
4 usually used as membrane-like materials, which can be beneficial to catalysis, as discussed
5 above. To date, electrospun materials have been mostly used for environmental catalytic
6 applications, like hexavalent chromium (Cr^{VI}) or nitro group reduction. Nevertheless, as-
7 prepared electrospun supports are not widely used as catalyst supports, as most reports in the
8 literature mentioned the use of the polymer mats as precursors for calcination for, as an
9 example, creating titania fibers. Most examples in the literature describe the use of polymer
10 fibers already containing chelating moieties like carboxylic acids or amines. Shi's group
11 described the use of polyethyleneimine (PEI) blended with poly(vinyl alcohol) (PVA) as mats
12 for the support of gold [148] and palladium [164] nanoparticles. Au NPs were used for the
13 successful reduction of nitro compounds, while Pd NPs were applied to the generation of Cr^{III}
14 from Cr^{VI} , which is highly carcinogenic. In the same way, Xiao's group used a blend of
15 poly(acrylic acid) (PAA) and PVA to chelate *in-situ* generated (sodium borohydride as
16 reducing agent) Ag NPs (**Fig. 9B**) for the catalytic reduction of *p*-nitrophenol [142] (**Table 8**).
17 Another interesting recent work is that from Pandey's team [140], who used electrospinning
18 to prepare poly(ether sulfone) (PES) fibers and took advantage of the presence of the ether
19 sulfone moieties to perform photolysis under UV irradiation to initiate the growth of
20 polyGMA chains. The pendant oxirane groups were then opened with hydrazine providing
21 directly attachment of the reducing agents on the support surface. A palladium salt was put in
22 contact with the fibers *via* an aqueous solution of palladium chloride and self-reduced. Hybrid
23 fibers were applied to the reduction of hexavalent chromium as well as *p*-nitrophenol (**Table**
24 **8**) but also the less common reduction of hexavalent uranium (U^{VI}) to U^{IV} .

1 Last but not least, one may mention the use of the double porogen templating approach
2 allowing for easily combining two levels of porosity and broadening the range of accessible
3 pore shape. Ly *et al.* recently designed doubly porous PHEMA-based materials as supports
4 for gold nanoparticles [105, 106] (**Fig. 9C**). They used fused NaCl particles as macroporogens
5 and isopropanol as a porogenic solvent for the production of the nanopores. The obtained
6 monoliths, *i.e.* monoporous with the higher porosity level, monoporous with the lower
7 porosity level and biporous ones, have been thoroughly characterized through mercury
8 intrusion porosimetry by using the Washburn equation (**Equation 1**). Data gathered in this
9 study showed that average pore sizes of 42 μm , 9 μm , 40 μm , and 8 μm were obtained by
10 MIP for monoporous with the higher porosity level, monoporous with the lower porosity level
11 and biporous HEMA-based polymeric frameworks, respectively. More importantly, the
12 porosity ratio of such a biporous polymer was estimated to be 92 %, which could be of
13 upmost interest for heterogeneous supported catalysis applications. The surface of the
14 biporous polymers was chemically modified in order to have amines or thiols directly on the
15 surface. HAuCl_4 solution was used to load gold ions onto the surface and NaBH_4 was used as
16 a reducing agent. Reduction of 4-nitrophenol was performed in order to prove the catalytic
17 efficiency of the as-prepared hybrids. Differences in the size and/or distribution of the
18 nanoparticles were observed as a function of the nature of the chelating group ($-\text{NH}_2$ *vs.* $-\text{SH}$),
19 thus leading to differences in the reaction yields. It was shown that thiol functions led to
20 bigger nanoparticles, and also surprisingly to leaching of NPs. Monoporous materials were
21 also synthesized in order to highlight the superiority of such doubly porous materials. While
22 monomodal porous polymers, *i.e.* with macroporosity or nanoporosity only, showed rather
23 similar efficiency, the doubly porous homologues exhibited higher catalytic activity. The
24 higher density of nanoparticles associated with the latter along with their higher porosity

1 ratios as compared to the nanoporous and macroporous materials were assumed to account for
2 such results (**Table 8**).

3

4 **4 Critical appraisal of the different strategies**

5 This review presented a critically selected overview of the various polymeric materials
6 so far implemented as potential supports for the adsorption of metallic nanoparticles meant for
7 supported heterogeneous catalysis. Each of these systems has inherent advantages/drawbacks
8 depending on their preparation conditions, *etc.* This section will bring a critical appraisal of
9 the different porous polymeric systems in terms of preparation, main characteristics, catalytic
10 properties, durability, *etc.* and of the related hybrid systems and their catalytic properties.

11 Fused silica capillaries filled with polymer monoliths are easy to prepare, dynamic loading of
12 the reactants in such microsystems being an undeniable advantage for the successful
13 functionalization of the pore surface with chemical grafts of interest and successive
14 immobilization of metallic nanoparticles through the *in situ* or *ex situ* strategies. In this way,
15 each preparation step is completed in a few hours or even in a few minutes. Supported
16 catalytic reactions operated in flow-through conditions have the major advantage to directly
17 give the desired product, without the need for any further purification step, provided of course
18 that no byproduct(s) is (are) generated during the catalytic reaction. More interestingly, such
19 microsystems are supposed to be easily scaled up and might be used in automation processes,
20 as mentioned by Nikbin *et al.* [149], that is to say that a chromatographic-column sized
21 catalytic reactor would be able to do what a tiny in-capillary microreactor can do. Such a
22 scale-up process would definitely solve the major issue regarding in-capillary monolithic
23 hybrid reactors, such as slow flow rates (about a few $\mu\text{L}\cdot\text{min}^{-1}$) due to rather high
24 backpressures and limited quantities of reactants that can be converted, *i.e.* generally a few
25 milligrams, due to microcolumns size/volume. Too high backpressures dramatically decrease

1 the lifetime of the column, reducing its reusability/durability. Moreover, such important
2 backpressure phenomena might lead to a higher leaching of adsorbed metallic nanoparticles,
3 which would be detrimental to further flow-through supported catalytic processes.

4 Nanoporous polymers arising from diblock copolymers can lead to different controlled
5 accessible morphologies (from cylinders to gyroids or to lamellae), thus enabling to tune the
6 porosity of the support. Nevertheless, a non-negligible series of not trivial synthetic steps is
7 required to produce them, which could be detrimental for their transfer to industrial processes.

8 Besides, depending on the alignment procedure and on the quantities of copolymer needed,
9 the orientation procedure time can be dramatically increased. For channel die processing, a
10 few hundreds of milligrams of copolymers are required to determine the best orientation
11 conditions, while for solvent vapour annealing, a diluted copolymer solution is enough for
12 film nanostructuration on silicon wafers. Yet, there is no widespread use of these nanoporous
13 materials for catalysis purposes.

14 Polymeric membranes seem to be the candidates of choice for efficient supported catalytic
15 reactions. However, some drawbacks could be found [170]. First, they need a specifically
16 designed and optimized reactor. Unfortunately, the production costs for a specific reactor
17 chamber must be added to the efforts for creating catalytic membranes, which are not trivial.

18 Moreover, as with capillary-based microreactors, a specific adjustment of the flow rate of
19 reactant solution to reach optimized reaction rates is necessary. Finally, one should keep in
20 mind that polymeric membranes are known to have a limited durability, depending especially
21 on their thermal, chemical, and mechanical properties. Indeed, the harsher the catalytic
22 reaction conditions, the quicker they degrade, adding higher costs of renewal, even if some
23 improvements have been achieved regarding the durability of such polymer-based
24 membranes.

1 Microporous networks have one major advantage, namely their specific surface area. Indeed,
2 the pores consist in voids generated by the monomer assembly, and are in the micropore
3 range. This could logically lead to catalytic supports declined for reactions in the gas phase.
4 Yet, examples of catalytic reactions in liquid media still exist with such polymer-based
5 microporous supports. However, they have a low permeability, and this is especially true for
6 pure carbon-based networks [171]. This limitation could notably prevent catalytic reactions
7 from occurring efficiently.

8 PolyHIPEs display a really well-accessible high porosity with interconnected pores that
9 enable high flow-through processes. However, since the void size is large (cavities are in the
10 tens/hundreds of micrometers range), specific surface areas are quite low [172]. Works
11 achieved by Sherrington's group attempted to overcome this issue [173], notably by using
12 porogenic solvents in addition to the HIPE process. However, resulting porous polymers
13 faced a new limitation, *i.e.* poor mechanical resistance of the monolith during flow-through
14 processes or even collapse of the porous structure.

15 Electrospun materials have risen since the mid 1990's, period during which such polymeric
16 fibers could be implemented for nanotechnology applications. As catalytic support, they offer
17 an interconnected porosity resulting from their engineering process. Moreover, they are
18 already used to prepared filtration membranes, which may lead to flow-through catalytic
19 reactors. Nevertheless, some limitations still exist. One may mention the difficulty to produce
20 uniform mats with a fiber diameter lower than 50 nm [174]. Indeed, a smaller diameter of
21 polymeric fiber would lead to a smaller volume of these fibers, thus enhancing the surface to
22 volume ratio. Progress is already on the way to overcome this issue by studying the solvent
23 evaporation during the electrospinning process, among others.

24 Finally, the double porogen approach affords high porosity ratios (> 90%) and interconnected
25 porosities, provided that the porogens are suitably chosen. However, further investigation still

1 needs to be performed to clearly correlate the pore morphology to the mass transfer properties
2 of the resulting materials. Very few of such doubly porous crosslinked polymers have been
3 used so far in the area of heterogeneous supported catalysis, only bringing limited information
4 in the field. Finally, no mechanical characterization data have been published yet on such
5 catalytic supports, which could bring some interesting information on their resistance to
6 different experimental conditions.

7

8 **5 Conclusions and prospects**

9 In conclusion, this review critically overviews the main types of polymers used as
10 potentially interesting supports for metallic nanoparticle immobilization. The as-prepared
11 hybrid materials seem to constitute candidates of choice in the area of heterogeneous
12 supported catalysis, as demonstrated by some notable works performed gathered in this
13 review article. Production costs for these porous polymers remain rather low, when compared
14 to their inorganic counterparts, while their preparation is rapid, making them suitable for
15 various applications, including heterogeneous supported catalysis. However, progress for
16 optimizing such polymer-based supports remains a milestone in order to optimize the
17 resulting hybrid materials. For instance, the optimization of specific surface area of such
18 porous polymers is of utmost importance, as it would definitely bring such organic materials
19 a step forward when compared to their inorganic counterparts. It was recently demonstrated
20 that HEMA-based porous polymers arising from reversed HIPes can be further
21 hypercrosslinked through a two-step synthetic pathway to generate porous polymers with
22 largely enhanced surface area of about $1500 \text{ m}^2 \cdot \text{g}^{-1}$ [175]. Another very promising research
23 area could rely on the development of porous metallic nanoparticles. Indeed, such nanometals
24 can develop a very large specific surface area, *e.g.* $8973 \text{ m}^2 \cdot \text{g}^{-1}$ for the outer surface area and
25 $58724 \text{ m}^2 \cdot \text{g}^{-1}$ for the inner surface area of 80 nm hollow porous gold nanoparticles, and thus

1 constitute promising candidates for the development of adsorbed catalysts at the surface of
2 porous polymers. The Holy Grail of such research area would rely on the preparation of
3 advanced hybrid systems that would be constituted of both high surface area counterparts, *i.e.*
4 porous nanometal and porous polymer support. Other morphologies of metallic nanoparticles
5 could also be largely envisioned as they could also lead to enhanced activities of the resulting
6 supported nanocatalysts [176].

7 Based on this overview concerning porous polymers meant for heterogeneous supported
8 catalysis, different key experimental parameters have to be indeed carefully taken into
9 consideration and especially porosity range and morphology of the materials as well as nature
10 of chemical moieties exposed at the pore surface so as to optimize the interactions between
11 the support and the metal (precursor). The catalytic processes involved, namely batch or flow-
12 through, but also the envisioned catalytic reaction are crucial parameters that matter for the
13 appropriate selection of the supports, notably regarding the stability and durability of the
14 hybrid systems in diverse experimental conditions (temperature, pressure, solvent nature,
15 *etc.*). Beyond the application of such hybrid systems in supported heterogeneous catalysis, it
16 is essential noticing that they could also be used as sensors or sorbents in analytical sciences,
17 filters for CO₂ sorption, or nanoreactors for the capture and release of biomolecules such as
18 cysteine-bearing peptides/proteins, for instance.

19

20

21 **Acknowledgments**

22 Financial support from CNRS and UPEC is gratefully acknowledged. The authors are
23 indebted to UPEC for providing R. Poupart with a Ph.D. grant.

24

1 **References**

2

- 3 [1] Van Leeuwen PW. *Homogeneous catalysis: understanding the art*: Springer Science &
4 Business Media; 2006.
- 5 [2] Widegren JA, Finke RG. A review of the problem of distinguishing true homogeneous
6 catalysis from soluble or other metal-particle heterogeneous catalysis under reducing
7 conditions. *J Mol Catal A: Chem* 2003; 198: 317-41.
- 8 [3] Herrmann WA, Kohlpaintner CW, Manetsberger RB, Bahrmann H, Kottmann H. Water-
9 soluble metal complexes and catalysts. *J Mol Catal A: Chem* 1995; 97: 65-72.
- 10 [4] Pirkanniemi K, Sillanpää M. Heterogeneous water phase catalysis as an environmental
11 application: a review. *Chemosphere* 2002; 48: 1047-60.
- 12 [5] Bell AT. The Impact of Nanoscience on Heterogeneous Catalysis. *Science* 2003; 299:
13 1688.
- 14 [6] Copéret C, Chabanas M, Petroff Saint-Arroman R, Basset J-M. Homogeneous and
15 Heterogeneous Catalysis: Bridging the Gap through Surface Organometallic Chemistry.
16 *Angew Chem Int Ed* 2003; 42: 156-81.
- 17 [7] Lu A-H, Salabas EL, Schüth F. Magnetic Nanoparticles: Synthesis, Protection,
18 Functionalization, and Application. *Angew Chem Int Ed* 2007; 46: 1222-44.
- 19 [8] Sachtler WMH, Zhang Z. Zeolite-Supported Transition Metal Catalysts*. In: D.D. Eley
20 HP, Paul BW, editors. *Advances in Catalysis*: Academic Press; 1993. p. 129-220.
- 21 [9] Opanasenko M, Stepnicka P, Cejka J. Heterogeneous Pd catalysts supported on silica
22 matrices. *RSC Adv* 2014; 4: 65137-62.
- 23 [10] Zhao D, Huo Q, Feng J, Chmelka BF, Stucky GD. Nonionic Triblock and Star Diblock
24 Copolymer and Oligomeric Surfactant Syntheses of Highly Ordered, Hydrothermally Stable,
25 Mesoporous Silica Structures. *J Am Chem Soc* 1998; 120: 6024-36.
- 26 [11] Wildgoose GG, Banks CE, Compton RG. Metal Nanoparticles and Related Materials
27 Supported on Carbon Nanotubes: Methods and Applications. *Small* 2006; 2: 182-93.
- 28 [12] Liu J, Chen L, Cui H, Zhang J, Zhang L, Su C-Y. Applications of metal-organic
29 frameworks in heterogeneous supramolecular catalysis. *Chem Soc Rev* 2014; 43: 6011-61.
- 30 [13] Vikrant K, Kumar V, Kim K-H, Kukkar D. Metal-organic frameworks (MOFs):
31 potential and challenges for capture and abatement of ammonia. *J Mater Chem A* 2017; 5:
32 22877-96.
- 33 [14] Wu D, Xu F, Sun B, Fu R, He H, Matyjaszewski K. Design and Preparation of Porous
34 Polymers. *Chem Rev* 2012; 112: 3959-4015.
- 35 [15] Seidl J, Malinský J, Dušek K, Heitz W. Makroporöse Styrol-Divinylbenzol-Copolymere
36 und ihre Verwendung in der Chromatographie und zur Darstellung von Ionenaustauschern.
37 *Fortschritte der Hochpolymeren-Forschung*. Berlin, Heidelberg: Springer Berlin Heidelberg;
38 1967. p. 113-213.
- 39 [16] Svec F, Fréchet JMJ. New Designs of Macroporous Polymers and Supports: From
40 Separation to Biocatalysis. *Science* 1996; 273: 205-11.
- 41 [17] Svec F, Fréchet JMJ. Modified poly(glycidyl methacrylate-co-ethylene dimethacrylate)
42 continuous rod columns for preparative-scale ion-exchange chromatography of proteins. *J*
43 *Chromatogr A* 1995; 702: 89-95.
- 44 [18] Xu Y, Cao Q, Svec F, Fréchet JMJ. Porous Polymer Monolithic Column with Surface-
45 Bound Gold Nanoparticles for the Capture and Separation of Cysteine-Containing Peptides.
46 *Anal Chem* 2010; 82: 3352-8.
- 47 [19] Luo Q, Zou H, Xiao X, Guo Z, Kong L, Mao X. Chromatographic separation of proteins
48 on metal immobilized iminodiacetic acid-bound molded monolithic rods of macroporous
49 poly(glycidyl methacrylate-co-ethylene dimethacrylate). *J Chromatogr A* 2001; 926: 255-64.

- 1 [20] Floris P, Twamley B, Nesterenko PN, Paull B, Connolly D. Agglomerated polymer
2 monoliths with bimetallic nano-particles as flow-through micro-reactors. *Microchim Acta*
3 2012; 179: 149-56.
- 4 [21] Gusev I, Huang X, Horváth C. Capillary columns with in situ formed porous monolithic
5 packing for micro high-performance liquid chromatography and capillary
6 electrochromatography. *J Chromatogr A* 1999; 855: 273-90.
- 7 [22] Lv Y, Lin Z, Svec F. Hypercrosslinked Large Surface Area Porous Polymer Monoliths
8 for Hydrophilic Interaction Liquid Chromatography of Small Molecules Featuring
9 Zwitterionic Functionalities Attached to Gold Nanoparticles Held in Layered Structure. *Anal*
10 *Chem* 2012; 84: 8457-60.
- 11 [23] Xie S, Svec F, Fréchet MJ. Design of reactive porous polymer supports for high
12 throughput bioreactors: Poly(2-vinyl-4,4-dimethylazlactone-co-acrylamide-co-ethylene
13 dimethacrylate) monoliths. *Biotechnol Bioeng* 1999; 62: 30-5.
- 14 [24] Guerrouache M, Carbonnier B, Vidal-Madjar C, Millot M-C. In situ functionalization of
15 N-acryloxysuccinimide-based monolith for reversed-phase electrochromatography. *J*
16 *Chromatogr A* 2007; 1149: 368-76.
- 17 [25] Guerrouache M, Millot M-C, Carbonnier B. Functionalization of Macroporous Organic
18 Polymer Monolith Based on Succinimide Ester Reactivity for Chiral Capillary
19 Chromatography: A Cyclodextrin Click Approach. *Macromol Rapid Commun* 2009; 30: 109-
20 13.
- 21 [26] Guerrouache M, Millot MC, Carbonnier B. Capillary columns for reversed-phase CEC
22 prepared via surface functionalization of polymer monolith with aromatic selectors. *J Sep Sci*
23 2011; 34: 2271-8.
- 24 [27] Dao TTH, Guerrouache M, Carbonnier B. Thiol-yne Click Adamantane Monolithic
25 Stationary Phase for Capillary Electrochromatography. *Chin J Chem* 2012; 30: 2281-4.
- 26 [28] Tijnelyte I, Babinot J, Guerrouache M, Valincius G, Carbonnier B. Hydrophilic
27 monolith with ethylene glycol-based grafts prepared via surface confined thiol-ene click
28 photoaddition. *Polymer* 2012; 53: 29-36.
- 29 [29] Kebe SI, Ben Boubaker M, Guerrouache M, Carbonnier B. Thiol-ene click chemistry for
30 the design of diol porous monoliths with hydrophilic surface interaction ability: a capillary
31 electrochromatography study. *New J Chem* 2016; 40: 6916-23.
- 32 [30] Mekhalif T, Kebe SI, Guerrouache M, Belattar N, Millot MC, Carbonnier B. Novel
33 Monolithic Stationary Phase with Surface-Grafted Triphenyl Selector for Reversed-Phase
34 Capillary Electrochromatography. *Chromatographia* 2016; 79: 1333-41.
- 35 [31] Poupart R, Le Droumaguet B, Guerrouache M, Carbonnier B. Copper nanoparticles
36 supported on permeable monolith with carboxylic acid surface functionality: Stability and
37 catalytic properties under reductive conditions. *Mater Chem Phys* 2015; 163: 446-52.
- 38 [32] Lav T-X, Carbonnier B, Guerrouache M, Grande D. Porous polystyrene-based
39 monolithic materials templated by semi-interpenetrating polymer networks for capillary
40 electrochromatography. *Polymer* 2010; 51: 5890-4.
- 41 [33] Lav T-X, Grande D, Gaillet C, Guerrouache M, Carbonnier B. Porous Poly(styrene-co-
42 divinylbenzene) Neutral Monolith: From Design and Characterization to Reversed-Phase
43 Capillary Electrochromatography Applications. *Macromol Chem Phys* 2012; 213: 64-71.
- 44 [34] Zhang J, Wu L, Jing D, Ding J. A comparative study of porous scaffolds with cubic and
45 spherical macropores. *Polymer* 2005; 46: 4979-85.
- 46 [35] Le Droumaguet B, Lacombe R, Ly H-B, Guerrouache M, Carbonnier B, Grande D.
47 Engineering functional doubly porous PHEMA-based materials. *Polymer* 2014; 55: 373-9.
- 48 [36] Lin H-R, Kuo C-J, Yang CY, Shaw S-Y, Wu Y-J. Preparation of macroporous
49 biodegradable PLGA scaffolds for cell attachment with the use of mixed salts as porogen
50 additives. *J Biomed Mater Res* 2002; 63: 271-9.

- 1 [37] Chow KS, Khor E. Novel Fabrication of Open-Pore Chitin Matrixes. *Biomacromolecules*
2 2000; 1: 61-7.
- 3 [38] LaNasa SM, Hoeffcker IT, Bryant SJ. Presence of pores and hydrogel composition
4 influence tensile properties of scaffolds fabricated from well-defined sphere templates. *J*
5 *Biomed Mater Res B* 2011; 96B: 294-302.
- 6 [39] Apel P. Track etching technique in membrane technology. *Radiat Meas* 2001; 34: 559-
7 66.
- 8 [40] Matsen MW, Bates FS. Unifying Weak- and Strong-Segregation Block Copolymer
9 Theories. *Macromolecules* 1996; 29: 1091-8.
- 10 [41] Bates FS, Fredrickson G. Block copolymers-designer soft materials. *Physics Today*
11 1999; 52: 32-8.
- 12 [42] Cochran EW, Garcia-Cervera CJ, Fredrickson GH. Stability of the Gyroid Phase in
13 Diblock Copolymers at Strong Segregation. *Macromolecules* 2006; 39: 2449-51.
- 14 [43] Lynd NA, Hillmyer MA. Influence of polydispersity on the self-assembly of diblock
15 copolymers. *Macromolecules* 2005; 38: 8803-10.
- 16 [44] Lee JS, Hirao A, Nakahama S. Polymerization of monomers containing functional silyl
17 groups. 5. Synthesis of new porous membranes with functional groups. *Macromolecules*
18 1988; 21: 274-6.
- 19 [45] Grande D, Le Droumaguet B. Design of functional nanoporous polymeric materials from
20 self-organized block copolymers. . In: Morton T, editor. *Nanopores and nanoporous materials*:
21 Nova Science Publishers; 2016. p. 1-26.
- 22 [46] Gorzolnik B, Davidson P, Beurroies I, Denoyel R, Grande D. Novel Functional
23 Mesoporous Materials Obtained from Nanostructured Diblock Copolymers. *Macromol Symp*
24 2010; 287: 127-34.
- 25 [47] Gorzolnik B, Penelle J, Grande D. Design of Mesoporous Materials with Controlled
26 Porosity and Functionality from Nanostructured Diblock Copolymers. *Polym Mater: Sci Eng*
27 2007; 97: 223-4.
- 28 [48] Chuma A, Horn HW, Swope WC, Pratt RC, Zhang L, Lohmeijer BGG, et al. The
29 Reaction Mechanism for the Organocatalytic Ring-Opening Polymerization of L-Lactide
30 Using a Guanidine-Based Catalyst: Hydrogen-Bonded or Covalently Bound? *J Am Chem Soc*
31 2008; 130: 6749-54.
- 32 [49] Cross ED, Allan LEN, Decken A, Shaver MP. Aluminum salen and salan complexes in
33 the ring-opening polymerization of cyclic esters: Controlled immortal and copolymerization
34 of rac- β -butyrolactone and rac-lactide. *J Polym Sci, Part A: Polym Chem* 2013; 51: 1137-46.
- 35 [50] Zalusky AS, Olayo-Valles R, Taylor CJ, Hillmyer MA. Mesoporous Polystyrene
36 Monoliths. *J Am Chem Soc* 2001; 123: 1519-20.
- 37 [51] Grande D, Penelle J, Davidson P, Beurroies I, Denoyel R. Functionalized ordered
38 nanoporous polymeric materials: From the synthesis of diblock copolymers to their
39 nanostructuration and their selective degradation. *Microporous Mesoporous Mater* 2011; 140:
40 34-9.
- 41 [52] Majdoub R, Antoun T, Droumaguet BL, Benzina M, Grande D. Original route to
42 polylactide-polystyrene diblock copolymers containing a sulfonyl group at the junction
43 between both blocks as precursors to functional nanoporous materials. *React Funct Polym*
44 2012; 72: 495-502.
- 45 [53] Sarkar A, Stefik M. Robust porous polymers enabled by a fast trifluoroacetic acid etch
46 with improved selectivity for polylactide. *Materials Chemistry Frontiers* 2017; 1: 1526-33.
- 47 [54] Kuhn P, Antonietti M, Thomas A. Porous, Covalent Triazine-Based Frameworks
48 Prepared by Ionothermal Synthesis. *Angew Chem Int Ed* 2008; 47: 3450-3.

1 [55] Goldbach JT, Russell TP, Penelle J. Synthesis and Thin Film Characterization of
2 Poly(styrene-block-methyl methacrylate) Containing an Anthracene Dimer Photocleavable
3 Junction Point. *Macromolecules* 2002; 35: 4271-6.

4 [56] Yurt S, Anyanwu UK, Scheintaub JR, Coughlin EB, Venkataraman D. Scission of
5 Diblock Copolymers into Their Constituent Blocks. *Macromolecules* 2006; 39: 1670-2.

6 [57] Zhang M, Yang L, Yurt S, Misner MJ, Chen JT, Coughlin EB, et al. Highly Ordered
7 Nanoporous Thin Films from Cleavable Polystyrene-block-poly(ethylene oxide). *Adv Mater*
8 2007; 19: 1571-6.

9 [58] Kang M, Moon B. Synthesis of Photocleavable Poly(styrene-block-ethylene oxide) and
10 Its Self-Assembly into Nanoporous Thin Films. *Macromolecules* 2009; 42: 455-8.

11 [59] Schumers J-M, Gohy J-F, Fustin C-A. A versatile strategy for the synthesis of block
12 copolymers bearing a photocleavable junction. *Polym Chem* 2010; 1: 161-3.

13 [60] Zhao H, Gu W, Sterner E, Russell TP, Coughlin EB, Theato P. Highly Ordered
14 Nanoporous Thin Films from Photocleavable Block Copolymers. *Macromolecules* 2011; 44:
15 6433-40.

16 [61] Gamys CG, Schumers J-M, Vlad A, Fustin C-A, Gohy J-F. Amine-functionalized
17 nanoporous thin films from a poly(ethylene oxide)-block-polystyrene diblock copolymer
18 bearing a photocleavable o-nitrobenzyl carbamate junction. *Soft Matter* 2012; 8: 4486-93.

19 [62] Ouchi M, Konishi A, Takenaka M, Sawamoto M. Consecutive living polymerization
20 from cationic to radical: a straightforward yet versatile methodology for the precision
21 synthesis of "cleavable" block copolymers with a hemiacetal ester junction. *Polym Chem*
22 2012; 3: 2193-9.

23 [63] Poupart R, Benlahoues A, Le Droumaguet B, Grande D. Porous Gold Nanoparticle-
24 Decorated Nanoreactors Prepared from Smartly Designed Functional Polystyrene-block-
25 Poly(D,L-Lactide) Diblock Copolymers: Toward Efficient Systems for Catalytic Cascade
26 Reaction Processes. *ACS Appl Mater Interfaces* 2017; 9: 31279-90.

27 [64] Satoh K, Poelma JE, Campos LM, Stahl B, Hawker CJ. A facile synthesis of clickable
28 and acid-cleavable PEO for acid-degradable block copolymers. *Polym Chem* 2012; 3: 1890-8.

29 [65] Goldbach JT, Lavery KA, Penelle J, Russell TP. Nano- to Macro-Sized Heterogeneities
30 Using Cleavable Diblock Copolymers. *Macromolecules* 2004; 37: 9639-45.

31 [66] Le Droumaguet B, Poupart R, Grande D. "Clickable" thiol-functionalized nanoporous
32 polymers: from their synthesis to further adsorption of gold nanoparticles and subsequent use
33 as efficient catalytic supports. *Polym Chem* 2015; 6: 8105-11.

34 [67] Ryu J-H, Park S, Kim B, Klaukherd A, Russell TP, Thayumanavan S. Highly Ordered
35 Gold Nanotubes Using Thiols at a Cleavable Block Copolymer Interface. *J Am Chem Soc*
36 2009; 131: 9870-1.

37 [68] Rao J, De S, Khan A. Synthesis and self-assembly of dynamic covalent block
38 copolymers: towards a general route to pore-functionalized membranes. *Chem Commun*
39 2012; 48: 3427-9.

40 [69] Glassner M, Blinco JP, Barner-Kowollik C. Formation of nanoporous materials via mild
41 retro-Diels-Alder chemistry. *Polym Chem* 2011; 2: 83-7.

42 [70] Fustin CA, Lohmeijer BGG, Duwez AS, Jonas AM, Schubert US, Gohy JF. Nanoporous
43 Thin Films from Self-Assembled Metallo- Supramolecular Block Copolymers. *Adv Mater*
44 2005; 17: 1162-5.

45 [71] Mugemana C, Gohy J-F, Fustin C-A. Functionalized Nanoporous Thin Films from
46 Metallo-Supramolecular Diblock Copolymers. *Langmuir* 2012; 28: 3018-23.

47 [72] Yu H, Stoffelbach F, Detrembleur C, Fustin C-A, Gohy J-F. Nanoporous thin films from
48 ionically connected diblock copolymers. *Eur Polym J* 2012; 48: 940-4.

1 [73] Montarnal D, Delbosc N, Chamignon C, Virolleaud M-A, Luo Y, Hawker CJ, et al.
2 Highly Ordered Nanoporous Films from Supramolecular Diblock Copolymers with
3 Hydrogen-Bonding Junctions. *Angew Chem Int Ed* 2015; 54: 11117-21.

4 [74] Zhao H, Gu W, Thielke MW, Sterner E, Tsai T, Russell TP, et al. Functionalized
5 Nanoporous Thin Films and Fibers from Photocleavable Block Copolymers Featuring
6 Activated Esters. *Macromolecules* 2013; 46: 5195-201.

7 [75] Dawson R, Cooper AI, Adams DJ. Nanoporous organic polymer networks. *Prog Polym*
8 *Sci* 2012; 37: 530-63.

9 [76] McKeown NB, Budd PM. Polymers of intrinsic microporosity (PIMs): organic materials
10 for membrane separations, heterogeneous catalysis and hydrogen storage. *Chem Soc Rev*
11 2006; 35: 675-83.

12 [77] Sakaushi K, Antonietti M. Carbon- and Nitrogen-Based Organic Frameworks. *Acc Chem*
13 *Res* 2015; 48: 1591-600.

14 [78] Shen C, Yu H, Wang Z. Synthesis of 1,3,5,7-tetrakis(4-cyanatophenyl)adamantane and
15 its microporous polycyanurate network for adsorption of organic vapors, hydrogen and carbon
16 dioxide. *Chem Commun* 2014; 50: 11238-41.

17 [79] Zhang Y, Riduan SN, Ying JY. Microporous Polyisocyanurate and Its Application in
18 Heterogeneous Catalysis. *Chem Eur J* 2009; 15: 1077-81.

19 [80] Dey SK, de Sousa Amadeu N, Janiak C. Microporous polyurethane material for size
20 selective heterogeneous catalysis of the Knoevenagel reaction. *Chem Commun* 2016; 52:
21 7834-7.

22 [81] Carta M, Croad M, Bugler K, Msayib KJ, McKeown NB. Heterogeneous organocatalysts
23 composed of microporous polymer networks assembled by Tröger's base formation. *Polym*
24 *Chem* 2014; 5: 5262-6.

25 [82] Ben T, Ren H, Ma S, Cao D, Lan J, Jing X, et al. Targeted Synthesis of a Porous
26 Aromatic Framework with High Stability and Exceptionally High Surface Area. *Angew*
27 *Chem Int Ed* 2009; 48: 9457-60.

28 [83] Verde-Sesto E, Pintado-Sierra M, Corma A, Maya EM, de la Campa JG, Iglesias M, et
29 al. First Pre-Functionalised Polymeric Aromatic Framework from
30 Mononitrotetrakis(iodophenyl)methane and its Applications. *Chem Eur J* 2014; 20: 5111-20.

31 [84] Zeltinger J, Sherwood JK, Graham DA, Müller R, Griffith LG. Effect of pore size and
32 void fraction on cellular adhesion, proliferation, and matrix deposition. *Tissue Eng* 2001; 7:
33 557-72.

34 [85] Ruiz JAR, Marc-Tallon J, Pedros M, Dumon M. Two-step micro cellular foaming of
35 amorphous polymers in supercritical CO₂. *J Supercrit Fluids* 2011; 57: 87-94.

36 [86] Ly HB, Le Droumaguet B, Monchiet V, Grande D. Tailoring doubly porous poly(2-
37 hydroxyethyl methacrylate)-based materials via thermally induced phase separation. *Polymer*
38 2016; 86: 138-46.

39 [87] Huang Z-M, Zhang YZ, Kotaki M, Ramakrishna S. A review on polymer nanofibers by
40 electrospinning and their applications in nanocomposites. *Compos Sci Technol* 2003; 63:
41 2223-53.

42 [88] Formhals A. Process and apparatus for preparing artificial threads. USA1934.

43 [89] Reneker DH, Chun I. Nanometre diameter fibres of polymer, produced by
44 electrospinning. *Nanotechnology* 1996; 7: 216-23.

45 [90] Reneker DH, Yarin AL, Zussman E, Xu H. Electrospinning of Nanofibers from Polymer
46 Solutions and Melts. In: Aref H, van der Giessen E, editors. *Advances in Applied Mechanics*:
47 Elsevier; 2007. p. 43-346.

48 [91] Villarreal-Gómez LJ, Cornejo-Bravo JM, Vera-Graziano R, Grande D. Electrospinning
49 as a powerful technique for biomedical applications: a critically selected survey. *J Biomat Sci*,
50 *Polym Ed* 2016; 27: 157-76.

- 1 [92] Bognitzki M, Czado W, Frese T, Schaper A, Hellwig M, Steinhart M, et al.
2 Nanostructured Fibers via Electrospinning. *Adv Mater* 2001; 13: 70-2.
- 3 [93] Cameron NR, Sherrington DC. Non-aqueous high internal phase emulsions. Preparation
4 and stability. *J Chem Soc, Faraday Trans* 1996; 92: 1543-7.
- 5 [94] Silverstein MS, Cameron NR. PolyHIPEs — Porous Polymers from High Internal Phase
6 Emulsions. *Encyclopedia of Polymer Science and Technology: John Wiley & Sons, Inc.;*
7 2002.
- 8 [95] Barby D, Haq Z. Low density porous cross-linked polymeric materials and their
9 preparation. *Google Patents*; 1982.
- 10 [96] Krajnc P, Brown JF, Cameron NR. Monolithic Scavenger Resins by Amine
11 Functionalizations of Poly(4-vinylbenzyl chloride-co-divinylbenzene) PolyHIPE Materials.
12 *Org Lett* 2002; 4: 2497-500.
- 13 [97] Krajnc P, Štefanec D, Pulko I. Acrylic Acid “Reversed” PolyHIPEs. *Macromol Rapid*
14 *Commun* 2005; 26: 1289-93.
- 15 [98] Kot E, Shirshova N, Bismarck A, Steinke JHG. Non-aqueous high internal phase
16 emulsion templates for synthesis of macroporous polymers in situ filled with cyclic carbonate
17 electrolytes. *RSC Adv* 2014; 4: 11512-9.
- 18 [99] R. Cameron N, C. Sherrington D. Preparation and glass transition temperatures of
19 elastomeric PolyHIPE materials. *J Mater Chem* 1997; 7: 2209-12.
- 20 [100] Féral-Martin C, Birot M, Deleuze H, Desforges A, Backov R. Integrative chemistry
21 toward the first spontaneous generation of gold nanoparticles within macrocellular polyHIPE
22 supports (Au@polyHIPE) and their application to eosin reduction. *React Funct Polym* 2007;
23 67: 1072-82.
- 24 [101] Mehraban M, Zadhoush A, Abdolkarim Hosseini Ravandi S, Bagheri R, Heidarkhan
25 Tehrani A. Preparation of porous nanofibers from electrospun polyacrylonitrile/calcium
26 carbonate composite nanofibers using porogen leaching technique. *J Appl Polym Sci* 2013;
27 128: 926-33.
- 28 [102] Ly H-B, Le Droumaguet B, Monchiet V, Grande D. Designing and modeling doubly
29 porous polymeric materials. *Eur Phys J Spec Top* 2015; 224: 1689-706.
- 30 [103] Ly HB, Le Droumaguet B, Monchiet V, Grande D. Facile fabrication of doubly porous
31 polymeric materials with controlled nano- and macro-porosity. *Polymer* 2015; 78: 13-21.
- 32 [104] Ly HB, Halbardier L, Grande D. Biporous Crosslinked Polymers With Controlled Pore
33 Size and Connectivity. *Macromol Symp* 2016; 365: 49-58.
- 34 [105] Ly HB, Poupart R, Halbardier L, Grande D. Functionalized Doubly Porous Networks:
35 From Synthesis to Application in Heterogeneous Catalysis. *Macromol Symp* 2016; 365: 40-8.
- 36 [106] Ly HB, Poupart R, Carbonnier B, Monchiet V, Le Droumaguet B, Grande D. Versatile
37 functionalization platform of biporous poly(2-hydroxyethyl methacrylate)-based materials:
38 Application in heterogeneous supported catalysis. *React Funct Polym* 2017; 121: 91-100.
- 39 [107] Webb PA, Orr C. Analytical methods in fine particle technology: *Micromeritics*
40 *Instrument Corp*; 1997.
- 41 [108] Washburn EW. Note on a Method of Determining the Distribution of Pore Sizes in a
42 Porous Material. *Proc Natl Acad Sci USA* 1921; 7: 115-6.
- 43 [109] Moura MJ, Ferreira PJ, Figueiredo MM. Mercury intrusion porosimetry in pulp and
44 paper technology. *Powder Technol* 2005; 160: 61-6.
- 45 [110] Winslow DN. Advances in Experimental Techniques for Mercury Intrusion
46 Porosimetry. In: Matijević E, Good RJ, editors. *Surface and Colloid Science: Volume 13.*
47 Boston, MA: Springer US; 1984. p. 259-82.
- 48 [111] Rouquerol J, Avnir D, Fairbridge C, Everett D, Haynes J, Pernicone N, et al.
49 Recommendations for the characterization of porous solids (Technical Report). *Pure Appl*
50 *Chem* 1994; 66: 1739-58.

- 1 [112] Feller C, Schouller E, Thomas F, Rouiller J, Herbillon AJ. N₂-BET Specific Surface
2 Areas of Some Low Activity Clay Soils and Their Relationships With Secondary Constituents
3 and Organic Matter Contents. *Soil Sci* 1992; 153: 293-9.
- 4 [113] Kim KC, Yoon T-U, Bae Y-S. Applicability of using CO₂ adsorption isotherms to
5 determine BET surface areas of microporous materials. *Microporous Mesoporous Mater*
6 2016; 224: 294-301.
- 7 [114] Yanazawa H, Ohshika K, Matsuzawa T. Precision Evaluation in Kr Adsorption for
8 Small BET Surface Area Measurements of Less Than 1 m². *Adsorption* 2000; 6: 73-7.
- 9 [115] Brunauer S, Emmett PH, Teller E. Adsorption of Gases in Multimolecular Layers. *J Am*
10 *Chem Soc* 1938; 60: 309-19.
- 11 [116] Barrett EP, Joyner LG, Halenda PP. The Determination of Pore Volume and Area
12 Distributions in Porous Substances. I. Computations from Nitrogen Isotherms. *J Am Chem*
13 *Soc* 1951; 73: 373-80.
- 14 [117] Iza M, Woerly S, Danumah C, Kaliaguine S, Bousmina M. Determination of pore size
15 distribution for mesoporous materials and polymeric gels by means of DSC measurements:
16 thermoporometry. *Polymer* 2000; 41: 5885-93.
- 17 [118] Brun M, Lallemand A, Quinson J-F, Eyraud C. A new method for the simultaneous
18 determination of the size and shape of pores: the thermoporometry. *Thermochim Acta* 1977;
19 21: 59-88.
- 20 [119] Jones BH, Lodge TP. Nanoporous Materials Derived from Polymeric Bicontinuous
21 Microemulsions. *Chem Mater* 2010; 22: 1279-81.
- 22 [120] Wulff M. Pore size determination by thermoporometry using acetonitrile. *Thermochim*
23 *Acta* 2004; 419: 291-4.
- 24 [121] Strange JH, Mitchell J, Webber JBW. Pore surface exploration by NMR. *Magn Reson*
25 *Imaging* 2003; 21: 221-6.
- 26 [122] Dlapka M, Danninger H, Gierl C, Lindqvist B. Defining the pores in PM components.
27 *Metal Powder Report* 2010; 65: 30-3.
- 28 [123] Vakifahmetoglu C, Colombo P. A Direct Method for the Fabrication of Macro-Porous
29 SiOC Ceramics from Pre-ceramic Polymers. *Adv Eng Mater* 2008; 10: 256-9.
- 30 [124] Moreno-Mañas M, Pleixats R. Formation of Carbon–Carbon Bonds under Catalysis by
31 Transition-Metal Nanoparticles. *Acc Chem Res* 2003; 36: 638-43.
- 32 [125] Astruc D, Lu F, Aranzas JR. Nanoparticles as Recyclable Catalysts: The Frontier
33 between Homogeneous and Heterogeneous Catalysis. *Angew Chem Int Ed* 2005; 44: 7852-
34 72.
- 35 [126] Takale BS, Bao M, Yamamoto Y. Gold nanoparticle (AuNPs) and gold nanopore
36 (AuNPore) catalysts in organic synthesis. *Org Biomol Chem* 2014; 12: 2005-27.
- 37 [127] Daniel M-C, Astruc D. Gold Nanoparticles: Assembly, Supramolecular Chemistry,
38 Quantum-Size-Related Properties, and Applications toward Biology, Catalysis, and
39 Nanotechnology. *Chem Rev* 2004; 104: 293-346.
- 40 [128] Gawande MB, Goswami A, Felpin F-X, Asefa T, Huang X, Silva R, et al. Cu and Cu-
41 Based Nanoparticles: Synthesis and Applications in Catalysis. *Chem Rev* 2016; 116: 3722-
42 811.
- 43 [129] Ranu BC, Dey R, Chatterjee T, Ahammed S. Copper Nanoparticle-Catalyzed
44 Carbon–Carbon and Carbon–Heteroatom Bond Formation with a Greener Perspective.
45 *ChemSusChem* 2012; 5: 22-44.
- 46 [130] Chen A, Holt-Hindle P. Platinum-Based Nanostructured Materials: Synthesis,
47 Properties, and Applications. *Chem Rev* 2010; 110: 3767-804.
- 48 [131] Astruc D. Palladium Nanoparticles as Efficient Green Homogeneous and
49 Heterogeneous Carbon–Carbon Coupling Precatalysts: A Unifying View. *Inorg Chem* 2007;
50 46: 1884-94.

1 [132] Munnik P, de Jongh PE, de Jong KP. Recent Developments in the Synthesis of
2 Supported Catalysts. *Chem Rev* 2015; 115: 6687-718.

3 [133] Wuithschick M, Paul B, Bienert R, Sarfraz A, Vainio U, Sztucki M, et al. Size-
4 Controlled Synthesis of Colloidal Silver Nanoparticles Based on Mechanistic Understanding.
5 *Chem Mater* 2013; 25: 4679-89.

6 [134] Wuithschick M, Witte S, Kettemann F, Rademann K, Polte J. Illustrating the formation
7 of metal nanoparticles with a growth concept based on colloidal stability. *Phys Chem Chem*
8 *Phys* 2015; 17: 19895-900.

9 [135] Wuithschick M, Birnbaum A, Witte S, Sztucki M, Vainio U, Pinna N, et al. Turkevich
10 in New Robes: Key Questions Answered for the Most Common Gold Nanoparticle Synthesis.
11 *ACS Nano* 2015; 9: 7052-71.

12 [136] Kettemann F, Birnbaum A, Witte S, Wuithschick M, Pinna N, Kraehnert R, et al.
13 Missing Piece of the Mechanism of the Turkevich Method: The Critical Role of Citrate
14 Protonation. *Chem Mater* 2016; 28: 4072-81.

15 [137] Boutonnet M, Kizling J, Stenius P, Maire G. The preparation of monodisperse colloidal
16 metal particles from microemulsions. *Colloid Surface* 1982; 5: 209-25.

17 [138] Shim I-W, Kim J-Y, Kim D-Y, Choi S. Preparation of Rh-containing polycarbonate
18 films and the study of their chemical properties in the polymer. *React Funct Polym* 2000; 43:
19 71-8.

20 [139] Groppo E, Agostini G, Borfecchia E, Wei L, Giannici F, Portale G, et al. Formation and
21 Growth of Pd Nanoparticles Inside a Highly Cross-Linked Polystyrene Support: Role of the
22 Reducing Agent. *J Phys Chem C* 2014; 118: 8406-15.

23 [140] Chappa S, Bharath RS, Oommen C, Pandey AK. Dual-Functional Grafted Electrospun
24 Polymer Microfiber Scaffold Hosted Palladium Nanoparticles for Catalyzing Redox
25 Reactions. *Macromol Chem Phys* 2017; 218: 1600555.

26 [141] Poupart R, Nour El Houda D, Chellapermal D, Guerrouache M, Carbonnier B, Le
27 Droumaguet B. Novel in-capillary polymeric monoliths arising from glycerol carbonate
28 methacrylate for flow-through catalytic and chromatographic applications. *RSC Adv* 2016; 6:
29 13614-7.

30 [142] Xiao S, Xu W, Ma H, Fang X. Size-tunable Ag nanoparticles immobilized in
31 electrospun nanofibers: synthesis, characterization, and application for catalytic reduction of
32 4-nitrophenol. *RSC Adv* 2012; 2: 319-27.

33 [143] Mora-Tamez L, Esquivel-Peña V, Ocampo AL, Rodríguez de San Miguel E, Grande D,
34 de Gyves J. Simultaneous Au^{III} Extraction and In Situ Formation of Polymeric Membrane-
35 Supported Au Nanoparticles: A Sustainable Process with Application in Catalysis.
36 *ChemSusChem* 2017; 10: 1482-93.

37 [144] Emin C, Remigy J-C, Lahitte J-F. Influence of UV grafting conditions and gel
38 formation on the loading and stabilization of palladium nanoparticles in photografted
39 polyethersulfone membrane for catalytic reactions. *J Membr Sci* 2014; 455: 55-63.

40 [145] Gu Y, Emin C, Remigy J-C, Favier I, Gómez M, Noble RD, et al. Hybrid Catalytic
41 Membranes: Tunable and Versatile Materials for Fine Chemistry Applications. *Mater Today-
42 Proc* 2016; 3: 419-23.

43 [146] Liu Y, Guerrouache M, Kebe SI, Carbonnier B, Le Droumaguet B. Gold nanoparticles-
44 supported histamine-grafted monolithic capillaries as efficient microreactors for flow-through
45 reduction of nitro-containing compounds. *J Mater Chem A* 2017; 5: 11805-14.

46 [147] Khalil AM, Georgiadou V, Guerrouache M, Mahouche-Chergui S, Dendrinou-Samara
47 C, Chehimi MM, et al. Gold-decorated polymeric monoliths: In-situ vs ex-situ immobilization
48 strategies and flow through catalytic applications towards nitrophenols reduction. *Polymer*
49 2015; 77: 218-26.

1 [148] Fang X, Ma H, Xiao S, Shen M, Guo R, Cao X, et al. Facile immobilization of gold
2 nanoparticles into electrospun polyethyleneimine/polyvinyl alcohol nanofibers for catalytic
3 applications. *J Mater Chem* 2011; 21: 4493-501.

4 [149] Nikbin N, Ladlow M, Ley SV. Continuous Flow Ligand-Free Heck Reactions Using
5 Monolithic Pd [0] Nanoparticles. *Org Process Res Dev* 2007; 11: 458-62.

6 [150] Bandari R, Höche T, Prager A, Dirnberger K, Buchmeiser MR. Ring-Opening
7 Metathesis Polymerization Based Pore-Size-Selective Functionalization of Glycidyl
8 Methacrylate Based Monolithic Media: Access to Size-Stable Nanoparticles for Ligand-Free
9 Metal Catalysis. *Chem Eur J* 2010; 16: 4650-8.

10 [151] Budarin VL, Clark JH, Luque R, Macquarrie DJ, White RJ. Palladium nanoparticles on
11 polysaccharide-derived mesoporous materials and their catalytic performance in C–C
12 coupling reactions. *Green Chem* 2008; 10: 382-7.

13 [152] Gu Y, Favier I, Pradel C, Gin DL, Lahitte J-F, Noble RD, et al. High catalytic
14 efficiency of palladium nanoparticles immobilized in a polymer membrane containing
15 poly(ionic liquid) in Suzuki–Miyaura cross-coupling reaction. *J Membr Sci* 2015; 492: 331-9.

16 [153] Gu Y, Bacchin P, Lahitte J-F, Remigy J-C, Favier I, Gómez M, et al. Catalytic
17 membrane reactor for Suzuki-Miyaura C–C cross-coupling: Explanation for its high
18 efficiency via modeling. *AIChE J* 2017; 63: 698-704.

19 [154] Zhang P, Weng Z, Guo J, Wang C. Solution-Dispersible, Colloidal, Conjugated Porous
20 Polymer Networks with Entrapped Palladium Nanocrystals for Heterogeneous Catalysis of
21 the Suzuki–Miyaura Coupling Reaction. *Chem Mater* 2011; 23: 5243-9.

22 [155] Du Z-L, Dang Q-Q, Zhang X-M. Heptazine-Based Porous Framework Supported
23 Palladium Nanoparticles for Green Suzuki–Miyaura Reaction. *Ind Eng Chem Res* 2017; 56:
24 4275-80.

25 [156] Desforges A, Backov R, Deleuze H, Mondain-Monval O. Generation of Palladium
26 Nanoparticles within Macrocellular Polymeric Supports: Application to Heterogeneous
27 Catalysis of the Suzuki–Miyaura Coupling Reaction. *Adv Funct Mater* 2005; 15: 1689-95.

28 [157] Bandari R, Prager A, Höche T, Buchmeiser MR. Formation of Pd-Nanoparticles within
29 the Pores of Ring Opening Metathesis Polymerization-Derived Polymeric Monoliths
30 for Use in Organometallic Catalysis. *ARKIVOC* 2011.

31 [158] Bandari R, Buchmeiser MR. Polymeric monolith supported Pt-nanoparticles as ligand-
32 free catalysts for olefin hydrosilylation under batch and continuous conditions. *Catal Sci*
33 *Technol* 2012; 2: 220-6.

34 [159] Poupart R, Le Droumaguet B, Guerrouache M, Grande D, Carbonnier B. Gold
35 nanoparticles immobilized on porous monoliths obtained from disulfide-based
36 dimethacrylate: Application to supported catalysis. *Polymer* 2017; 126: 455-62.

37 [160] Floris P, Twamley B, Nesterenko PN, Paull B, Connolly D. Fabrication and
38 characterisation of gold nano-particle modified polymer monoliths for flow-through catalytic
39 reactions and their application in the reduction of hexacyanoferrate. *Microchim Acta* 2014;
40 181: 249-56.

41 [161] Taori VP, Bandari R, Buchmeiser MR. Selective Reduction of CO₂ with Silanes over
42 Platinum Nanoparticles Immobilised on a Polymeric Monolithic Support under Ambient
43 Conditions. *Chem Eur J* 2014; 20: 3292-6.

44 [162] Desforges A, Deleuze H, Mondain-Monval O, Backov R. Palladium Nanoparticle
45 Generation within Microcellular Polymeric Foam and Size Dependence under Synthetic
46 Conditions. *Ind Eng Chem Res* 2005; 44: 8521-9.

47 [163] Gu YY, Remigy JC, Favier I, Gomez M, Noble RD, Lahitte JF. Membrane Reactor
48 Based on Hybrid Nanomaterials for Process Intensification of Catalytic Hydrogenation
49 Reaction: an Example of Reduction of the Environmental Footprint of Chemical Synthesis
50 from a Batch to a Continuous Flow Chemistry Process. In: Chianese A, DiPalma L, Petrucci

1 E, Stoller M, editors. International Conference on Nanotechnology Based Innovative
2 Applications for the Environment 2016. p. 367-72.

3 [164] Huang Y, Ma H, Wang S, Shen M, Guo R, Cao X, et al. Efficient Catalytic Reduction
4 of Hexavalent Chromium Using Palladium Nanoparticle-Immobilized Electrospun Polymer
5 Nanofibers. *ACS Appl Mater Interfaces* 2012; 4: 3054-61.

6 [165] Cao Q, Xu Y, Liu F, Svec F, Fréchet JMJ. Polymer Monoliths with Exchangeable
7 Chemistries: Use of Gold Nanoparticles As Intermediate Ligands for Capillary Columns with
8 Varying Surface Functionalities. *Anal Chem* 2010; 82: 7416-21.

9 [166] Connolly D, Twamley B, Paull B. High-capacity gold nanoparticle functionalised
10 polymer monoliths. *Chem Commun* 2010; 46: 2109-11.

11 [167] Guerrouache M, Mahouche-Chergui S, Chehimi MM, Carbonnier B. Site-specific
12 immobilisation of gold nanoparticles on a porous monolith surface by using a thiol-yne click
13 photopatterning approach. *Chem Commun* 2012; 48: 7486-8.

14 [168] Merino E, Verde-Sesto E, Maya EM, Corma A, Iglesias M, Sánchez F. Mono-
15 functionalization of porous aromatic frameworks to use as compatible heterogeneous catalysts
16 in one-pot cascade reactions. *Appl Catal, A* 2014; 469: 206-12.

17 [169] Xie Z, Wang C, deKrafft KE, Lin W. Highly Stable and Porous Cross-Linked Polymers
18 for Efficient Photocatalysis. *J Am Chem Soc* 2011; 133: 2056-9.

19 [170] Vankelecom IFJ. Polymeric Membranes in Catalytic Reactors. *Chem Rev* 2002; 102:
20 3779-810.

21 [171] Cheng G, Hasell T, Trewin A, Adams DJ, Cooper AI. Soluble Conjugated Microporous
22 Polymers. *Angew Chem Int Ed* 2012; 51: 12727-31.

23 [172] Cameron NR. High internal phase emulsion templating as a route to well-defined
24 porous polymers. *Polymer* 2005; 46: 1439-49.

25 [173] Hainey P, Huxham IM, Rowatt B, Sherrington DC, Tetley L. Synthesis and
26 ultrastructural studies of styrene-divinylbenzene Polyhipe polymers. *Macromolecules* 1991;
27 24: 117-21.

28 [174] Dzenis Y. Spinning Continuous Fibers for Nanotechnology. *Science* 2004; 304: 1917-9.

29 [175] Mezhoud S, Paljevac M, Koler A, Le Droumaguet B, Grande D, Krajnc P. Novel
30 hypercrosslinking approach toward high surface area functional 2-hydroxyethyl methacrylate-
31 based polyHIPEs. *React Funct Polym* 2018; 132: 51-9.

32 [176] Zeng J, Zhang Q, Chen J, Xia Y. A Comparison Study of the Catalytic Properties of
33 Au-Based Nanocages, Nanoboxes, and Nanoparticles. *Nano Lett* 2010; 10: 30-5.

34